Technical Report Documentation Page

1. Report No. ABC-UTC-2016-C2-FIU06	2. Government Accession No.	3. Recipient's Catalog No.	
4. Title and Subtitle **Laminated Wood Deck System for Folded Plate Girder**		5. Report Date February 2026 6. Performing Organization Code Florida International University	
7. Author(s) Muhammad Faheem Ud Din Afzal (https://orcid.org/0000-0002-6092-1990); Aaron Yakel (https://orcid.org/0000-0001-9007-4967); and Atorod Azizinamini (https://orcid.org/0000-0001-7627-6757)		8. Performing Organization Report No.	
9. Performing Organization Name and Address Department of Civil and Environmental Engineering Florida International University 10555 West Flagler Street, EC 3680 Miami, FL 33174		10. Work Unit No. (TRAIS) 11. Contract or Grant No. 69A3551747121	
12. Sponsoring Organization Name and Address Accelerated Bridge Construction University Transportation Center Florida International University 10555 W. Flagler Street, EC 3680 Miami, FL 33174 US Department of Transportation Office of the Assistant Secretary for Research and Technology And Federal Highway Administration 1200 New Jersey Avenue, SE Washington, DC 201590		13. Type of Report and Period Covered Final Report 14. Sponsoring Agency Code	
15. Supplementary Notes Visit www.abc-utc.fiu.edu for other ABC reports.			
16. Abstract Folded plate girder (FPG) is constructed using a steel sheet, which is bent using a bending machine to create box girder with an open bottom flange. FPG can be used in accelerated bridge construction (ABC) by casting a full-depth deck panel on top of the FPG while in a precast plant. Advantages of the proposed deck systems include accelerated construction if compared to cast-in-place construction. The scope of the research was modified to more fully address splicing of the FPG. Splicing the FPG makes it suitable for spans up to 100 ft., allowing more bridges to take advantage of such system. A large-scale specimen was tested under fatigue loading for service life design and under ultimate load for AASHTO strength design.			
17. Key Words Folded Plate Steel girder, Cyclic Loading, Fatigue testing, Connection testing, Direct welding, Accelerated Bridge Construction.		18. Distribution Statement No restrictions.	
19. Security Classification (of this report) Unclassified.	20. Security Classification (of this page) Unclassified.	21. No. of Pages 48	22. Price

(this page is intentionally left blank)

Laminated Wood Deck System for Folded Plate Girder

Final Report

February 2026

Principal Investigator: Atorod Azizinamini

Department of Civil and Environmental Engineering
Florida International University

Authors

Muhammad Faheem Ud Din Afzal
Aaron Yakel
Atorod Azizinamini

Sponsored by
Accelerated Bridge Construction University Transportation Center

A report from
Department of Civil and Environmental Engineering
Florida International University
10555 West Flagler Street, EC 3680
Miami, FL 33174
Phone: 305-348-2824 / Fax: 305-348-2802
https://cee.fiu.edu/

Disclaimer

The contents of this report reflect the views of the authors, who are responsible for the facts and the accuracy of the information presented herein. This document is disseminated in the interest of information exchange. The report is funded, partially or entirely, by a grant from the U.S. Department of Transportation's University Transportation Program. However, the U.S. Government assumes no liability for the contents or use thereof.

Contents

List of Figures

List of Tables

Acknowledgments

This project was supported by the Accelerated Bridge Construction University Transportation Center (ABC-UTC at www.abc-utc.fiu.edu) at Florida International University (FIU), as lead institution, University of Oklahoma (OU), University of Washington (UW), Iowa State University (ISU) and the University of Nevada-Reno (UNR) as partner institutions. The authors would like to acknowledge the ABC-UTC support.

The author would like to extend special appreciation to the ABC-UTC and the U.S. Department of Transportation Office of the Assistant Secretary for Research and Technology for funding this project.

The author would like to thank all the State DOTs that participated in the survey; this work would not have been possible without their participation.

The author would like to thank the Research Advisory Panel members: Ahmad Abu-Hawash (Iowa DOT), James Corney (Utah DOT), Romeo Garcia (FHWA), and Bruce Johnson (Oregon DOT).

CHAPTER 1: INTRODUCTION

Folded plate girder (FPG) is a superstructure bridge system that involves cold bending a box shape out of a single sheet with an open bottom flange. The cold bend eliminates the costly and inconsistent shop weld found in conventional steel girders. The FPG concept works for both conventional construction and accelerated bridge construction (ABC). In conventional construction, formwork is needed along with the placement of deck reinforcement then the concrete is placed. In ABC, a full-depth deck panel unit is fabricated in a precast planet of in fabrication yard near the bridge site with transverse steel reinforcing bars extended outside the cured slab portion to form closure joint with adjacent full-depth deck unit then ultra-high performance concrete (UHPC) or normal strength concrete is placed in closure joints.

Folded plate girders (FPGs) have a wide range of current uses in bridge construction. To date several states have used the system that includes Nebraska, Massachusetts, Montana, Pennsylvania, and Michigan. It is a proprietary bridge system specifically designed for accelerated bridge construction (ABC), allowing for quick assembly in conjunction with precast processes. Other advantages include removing the requirement of cross frames, easy to inspect and recently proven to be very competitive with other materials.

The FPG system was implemented in ABC using full-depth deck panels fabricated on top of the girder in Pennsylvania near Bradford as shown in Figure 1. The FPG can be bent using a large steel sheet in 20-30 minutes using a bending machine.

a 

Figure 1. Folded steel plate girder system bridge in Pennsylvania erected near Bradford.

One of the applications of the FPG in ABC involves casting full-depth deck panels on top of the girder. To further improve the efficiency of FPGs in ABC projects, alternative deck systems such as laminated wood, orthotropic decks, and prefabricated decks are being explored. These alternatives offer faster construction timelines compared to traditional cast-in-place methods.

1.1 Modification of Research Intent

As indicated by the title of the project and report, the research project intended to investigate a laminated wood deck system. However, with sponsor approval, the research was re-tasked with investigating a spliced FPG system suitable for extending the applicability up to 100 ft spans.

The PI just completed the fatigue testing of FPG specimen using concrete deck system suitable for 100 ft. spans. This progress report presents the results of this system. An ultimate test for this specimen was planned to be conducted in March 2020 but postponed due to COVID 19 outbreak. The proposed system for 100 ft. span length utilizes one of the two connections shown in Figure 2.

Figure 2. Two details to expand the span of FPG girder to 100 ft.

1.2 Problem Statement and Objectives

Due to the limitation of bending machine (press-brake) used to fabricate the girders, single-span bridges using FPG cannot extend beyond 60 ft.

The main objectives of this project are:

1- The original objective of this project was to develop new deck systems for FPG aiming at cost reduction and faster construction. However, the objective of this project was revised to include the results from fatigue and ultimate test conducted at FIU for the extended length of FPG.

2- Conduct proof of concept experimental work on a full-scale spliced FPG.

   a. Fatigue Loading

   b. Ultimate Load Test

CHAPTER 2: SUMMARY OF SPLICE DETAIL DEVELOPMENT

The main approach to extending the maximum length of FSPGBS is in the form of splicing Folded Plate girders with lengths of less than 60 ft. to form longer lengths. To keep the number of connections at a minimum, preference is to splice the two pieces in the middle. Another reason to splice the girders in the middle is to incorporate camber by cutting ends of the piece at slight angle and then connect the two pieces. An obvious adaptation would be to splice away from span centerline with either unbalanced lengths, or a three-segment arrangement. These would benefit from reduced demand at the splice location. For purposes of the investigation, a centrally spliced arrangement is more critical.

Three main connection types were envisioned, and series of non-linear finite element analysis were carried out to comprehend their behavior. Two classes of connection types were investigated - bolted and welded. Within each category, several variations were considered. Another connection alternative is directly welding the two pieces using full penetration welds this option did not require any analysis.

For each of the connection detail categories, numerous non-linear FEA were carried out and only select results are reported here for brevity.

2.1 Span Length Study

The investigation included conducting a parametric study to develop series of designs that could accommodate various span lengths exceeding 60 ft and up to 105 ft. Results of the study are shown in *Table 1.*

The main parameters varied in the design parametric study were the plate thickness and plate yield strength. For each span length several combinations were considered and for each combination, the following information is provided.

Demand to Capacity Ratios

- Maximum positive moment produced by load at Strength Limit State I divided by the Maximum Moment Capacity
- Maximum stress in bottom flange, at service limit state II, divided by the Allowable Stress service limit state II
- Maximum fatigue stress in the bottom flange divided by the Allowable stress for fatigue
- Maximum deflection divided by the Allowable deflection Limit

Values with a performance ratio below 1.0 (unity) indicate meeting the AASHTO requirements and are shaded green. As an example for a bridge with 80 ft simple span length, one could use the cross section shown above, ½ inch thick plate with 50 ksi yield strength.

The deflection criterion is optional; therefore, this value is shaded yellow when all other ratios are satisfied for a particular combination.

The far-left column indicates the preferred combination for spans of 80, 90, 95, and 105.

Table 1. Span Length Study

W44H34O16							
Unfolded L = 119 Inches							
	Span	Thickness	Yield	Pos Str	Service	Fatigue	Defl
	90	0.5	50	0.86	1.17	0.81	1.15
	85	0.5	50	0.79	1.08	0.76	1
80	80	0.5	50	0.73	0.99	0.71	0.92
	75	0.5	50				
	65	0.5	50				
95 Alt	95	0.5	70	0.73	0.9	0.86	1.29
90	90	0.5	70	0.67	0.84	0.81	1.15
	85	0.5	70				
	75	0.5	70				
	65	0.5	70				
	105	0.75	50	0.85	1.11	0.7	1.13
95	95	0.75	50	0.74	0.96	0.63	0.93
	85	0.75	50				
	75	0.75	50				
105	105	0.75	70	0.65	0.79	0.7	1.13
	95	0.75	70				
	85	0.75	70				
	75	0.75	70				

Figure 3 shows the cross-sectional geometry used in all analyses listed in table above as well as the details of the prototype bridge considered.

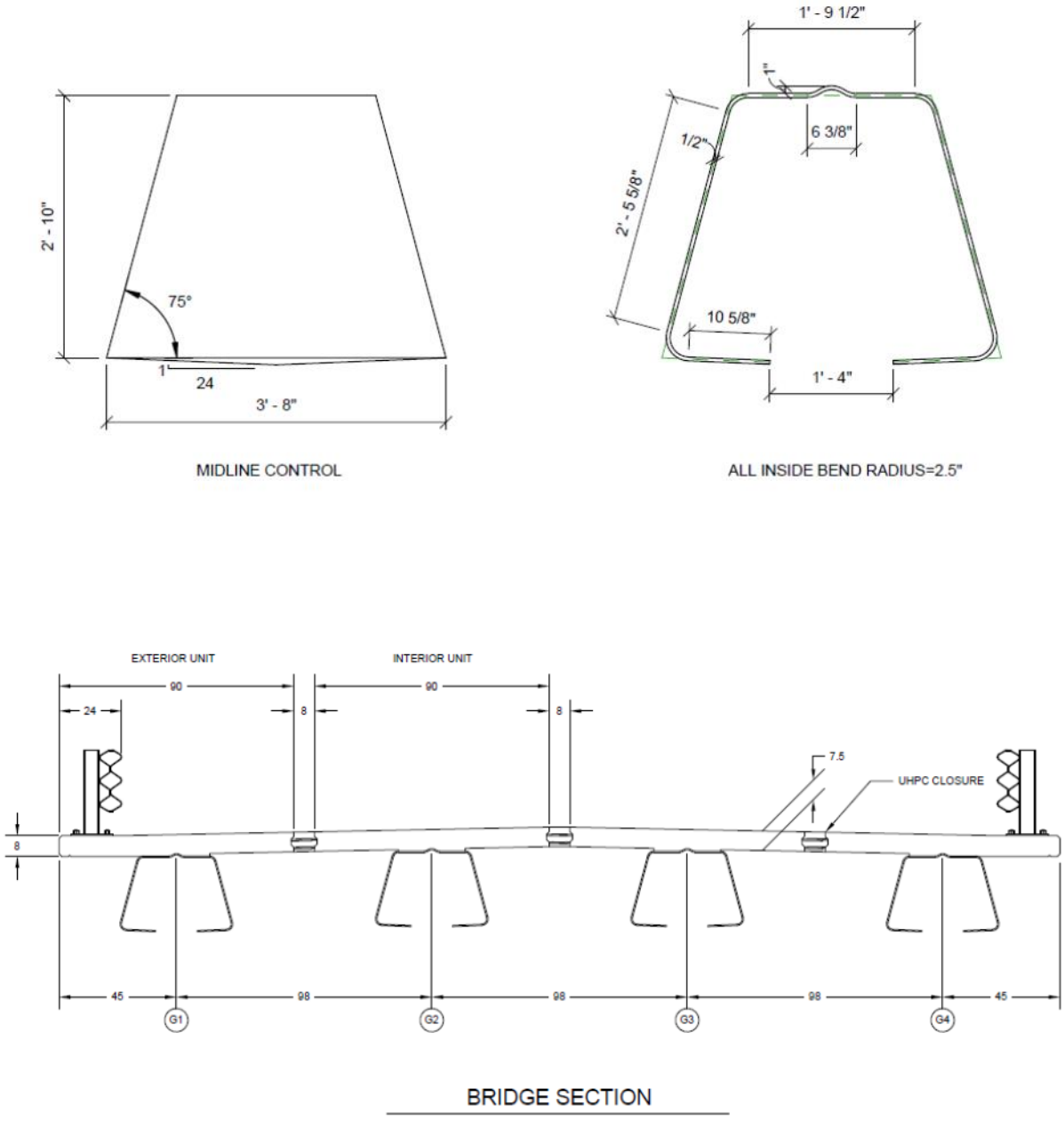

Figure 3. Prototype Bridge

Following is additional information related to span parametric study conducted. The distribution factors for flexure are 0.605 and 0.316 for strength and fatigue, respectively. The load values and resulting combinations are given in *Table 2*. The values assume shored (pre-topped) construction and a 2" future wearing surface plus a 10% miscellaneous steel factor.

Table 2. Loading Analysis Results

		STR I	STR 2X LL	SRV II	FAT I	FAT II
	(k-ft)	(k-ft)	(k-ft)	(k-ft)	(k-ft)	(k-ft)
DC	513	1.25	1.25	1		
DW	121	1.5	1.5	1		
DF(1.33TRK+LN)	888	1.75	3.5	1.3		
DF(1.15TRK)	237				1.5	0.75
		2377	3931	1788	356	178

2.2 Cast Tension Bar Connection

The first attempt was to consider the detail shown in *Figure 4*. In this concept, a concrete slab would be cast onto the bottom flange of the box to aid in the transfer of forces. The splice, occurring at the middle of a simply supported span, must resist tension at the bottom flange compression at the top.

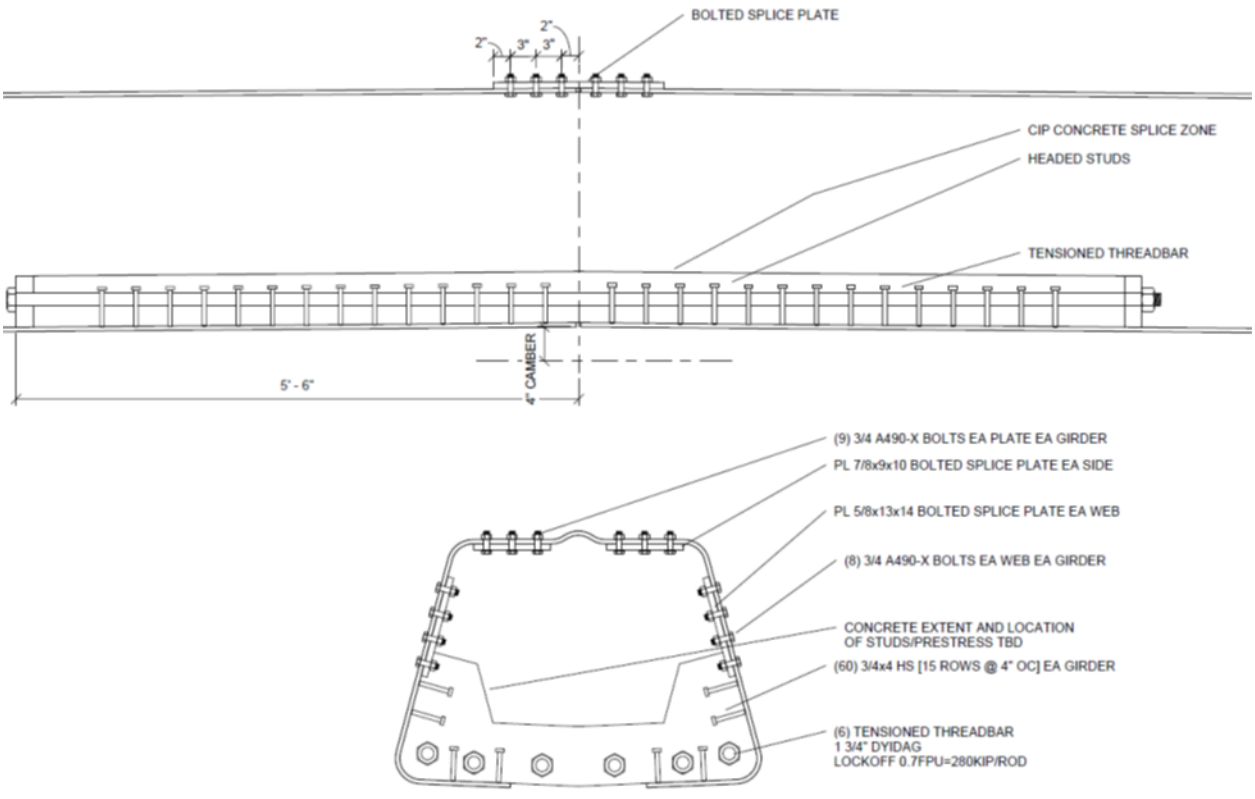

Figure 4. Cast thread bar splice detail

Shear studs attached to the bottom flange would provide for the connection to each girder, and post-tensioning along with possible mild reinforcement would tie the two together. This connection would provide the tension component of the force transfer. The deck would provide

the final compressive component. The girders would be attached to the deck with typical shear studs.

Bolted splice plates at the top flange and web provide for alignment of the elements and aid in the compressive force transfer. Depending on whether a shored or free spanning construction method was used, this connection may also support compressive loads during casting of the deck.

2.3 Direct Bolting

In an effort to develop a more efficient connection, investigations into a direct bolted alternative began next. A fill plate between the flanges was included to help distribute the load to the bolts near the center of the cross-section. The fill plate fills the gap between the flanges and provides additional length over which to spread the connection.

Initially, it was desired to keep all of the bolts on the exterior of the box to facilitate construction; *Figure 5* shows this arrangement. However, it was soon discovered that the large amount of force to be transferred required that the bolts be clustered at the bottom flange, both above and below the flange. If bolting was going to be required on the inside of the box for strength, then bolting at the webs would be placed to the inside as well for aesthetics, as shown in the second figure.

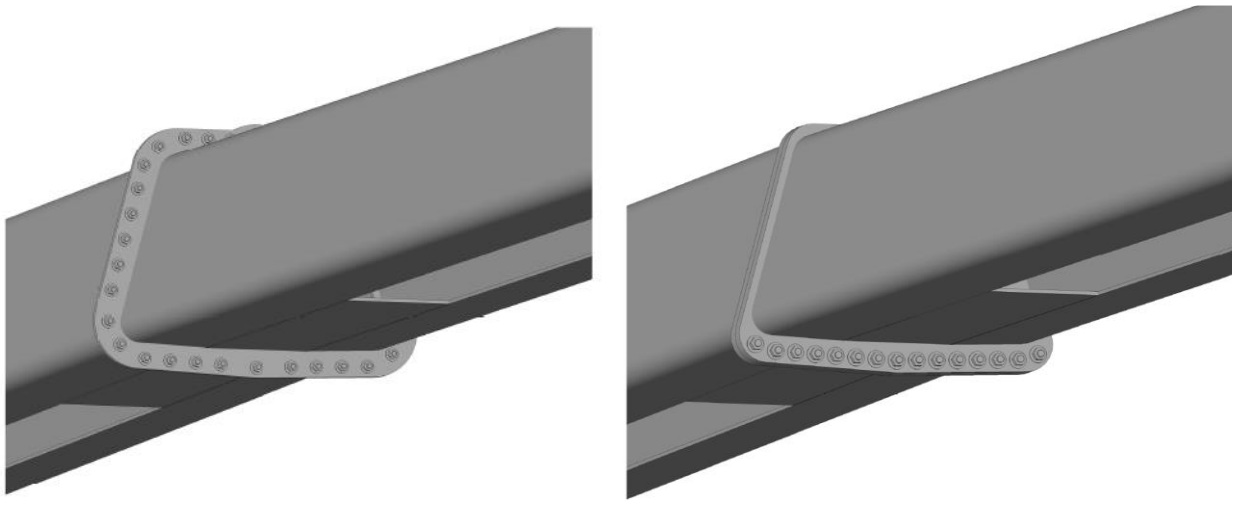

Exterior Bolts **Interior Bolts – Bottom Clustered**

Figure 5. Bolted Splice

The general-purpose finite element program ANSYS (benchtop interface) was used to analyze various connection details. Element selection and modeling techniques evolved over time.

The first models considered only one-half of a span, with a rigid interface representing the other span. In fact, the initial intent of the analysis was to investigate the demands on the base plate for the test setup. *Figure 6* shows the stress results from one of the early models.

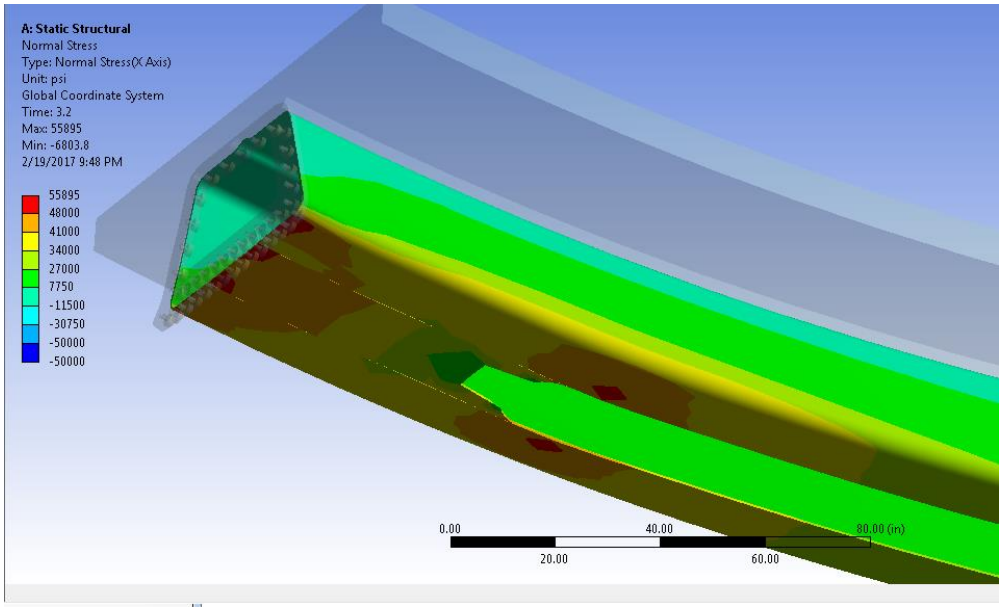

Figure 6. Preliminary Half-Span FEM Results

The global behavior of the model matched the hand calculated predicted values well. Early on, localized effects were observed and efforts were undertaken to reduce stress concentrations. The model shown above represents an early attempt at smoothing the transition to the fill plate. Note that the hotspot in the bottom flange is several inches away from the actual end of the fill plate. It has been found that the hotspot is due to both a stress concentration effect and a geometric restraint effect. If the box is continuous with nothing between the flanges, the flanges tend to move apart under vertical loading. The filler plate and connection plate restrains this movement, which creates tension on the inside face of the flange at the same location where the stress concentration occurs. This was observed by providing various levels of lateral restraint along the length of the flanges and comparing the results.

Figure 7 shows the final configuration that was chosen for the filler plate. The deep V shape reduces the lateral stiffness, thereby easing the stress riser due to the lateral restraint. From the elastic analysis, the fatigue stress was found to be 4 to 5 ksi. Under an ultimate loading pattern, nonlinearity was first observed at a load level corresponding to 1.5x live load.

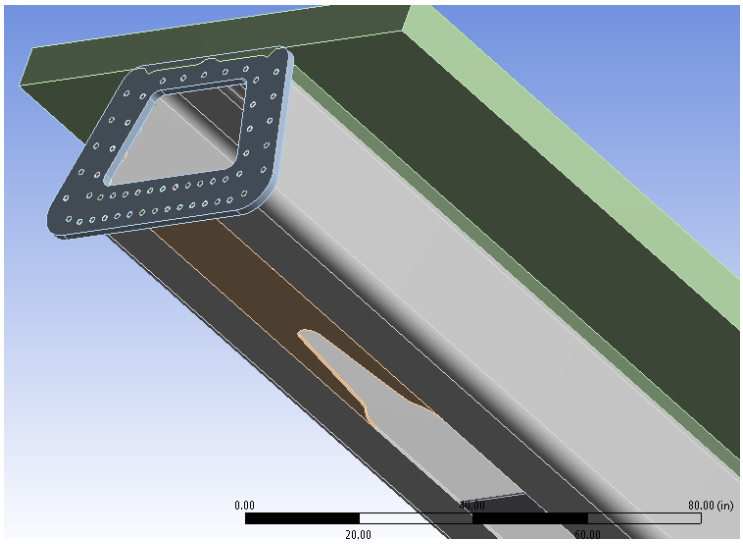

Figure 7. Keyhole Fill Plate

The moment-deflection curve for the bolted models is shown in *Figure 8*. Load levels corresponding to various conditions are also indicated in the figure.

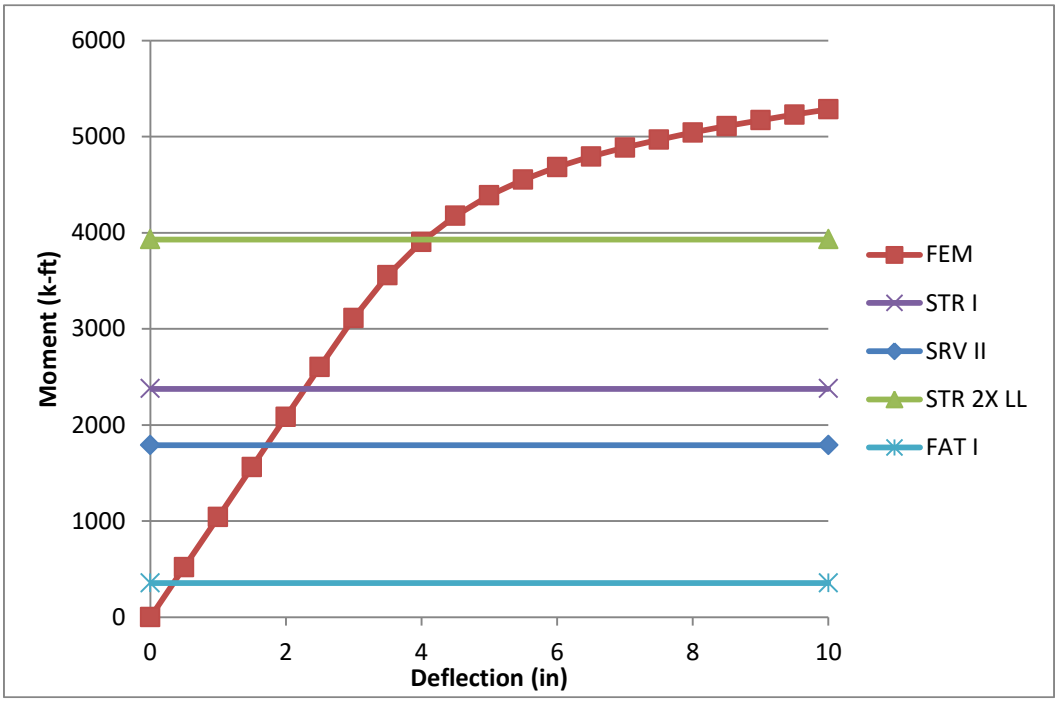

Figure 8. Moment Versus Applied Deflection

The factored and distributed moment at the Strength I load level is 2377 k-ft. The moment occurred at deflection level of 2.3 inches in the finite element model. *Figure 9* shows the stresses at the Strength I limit state.

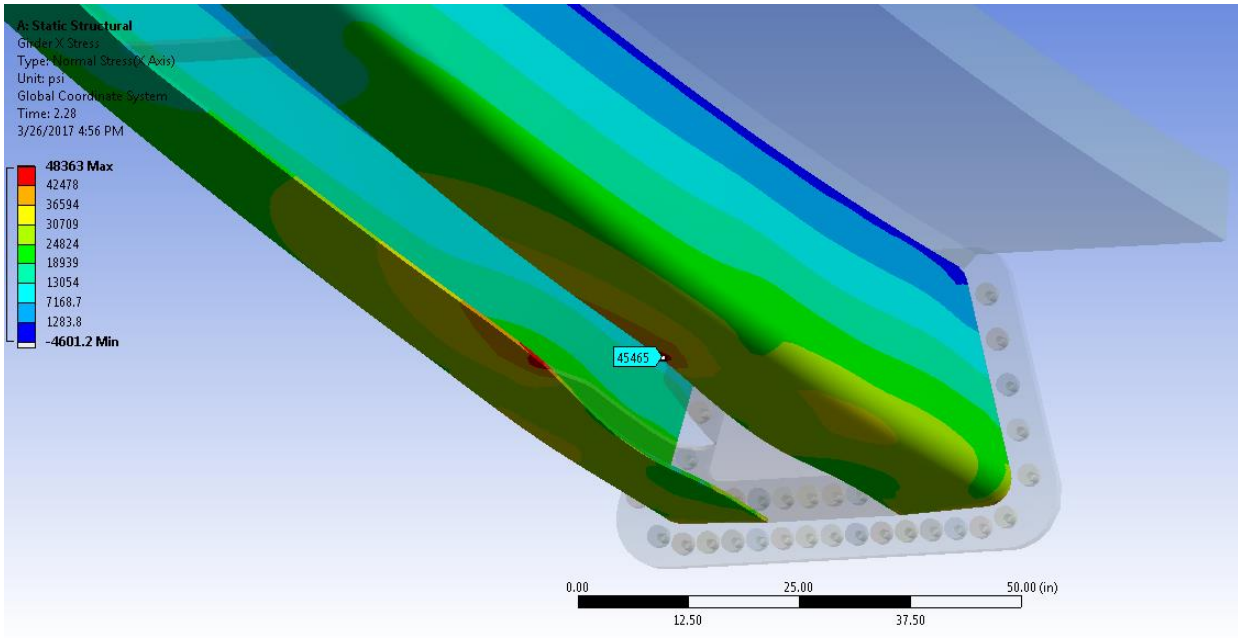

Figure 9. Strength I Stresses

2.4 Direct Weld

Due to the folded plate fabrication process, the manufacture of the folded plate girder has inherent uncertainties concerning geometry. The greatest advantage of the bolted connection was that misalignment between the flanges could be compensated for with the splice plates. After speaking with several fabricators, it was determined that similar alignment could be achieved with a direct weld process as well.

Figure 10 shows the initial direct weld concept. Each segment of girder is directly welded to a common splice plate. The analysis results indicated a significant stress concentration at the corner of the flange. Considerable effort was directed at smoothing the transition. A fillet plate was added to the inside of the flange to provide a radiused transition and the groove weld at the plate was built out and radiused. However, it was eventually determined that none of these measures lowered the stress concentrations to an acceptable range.

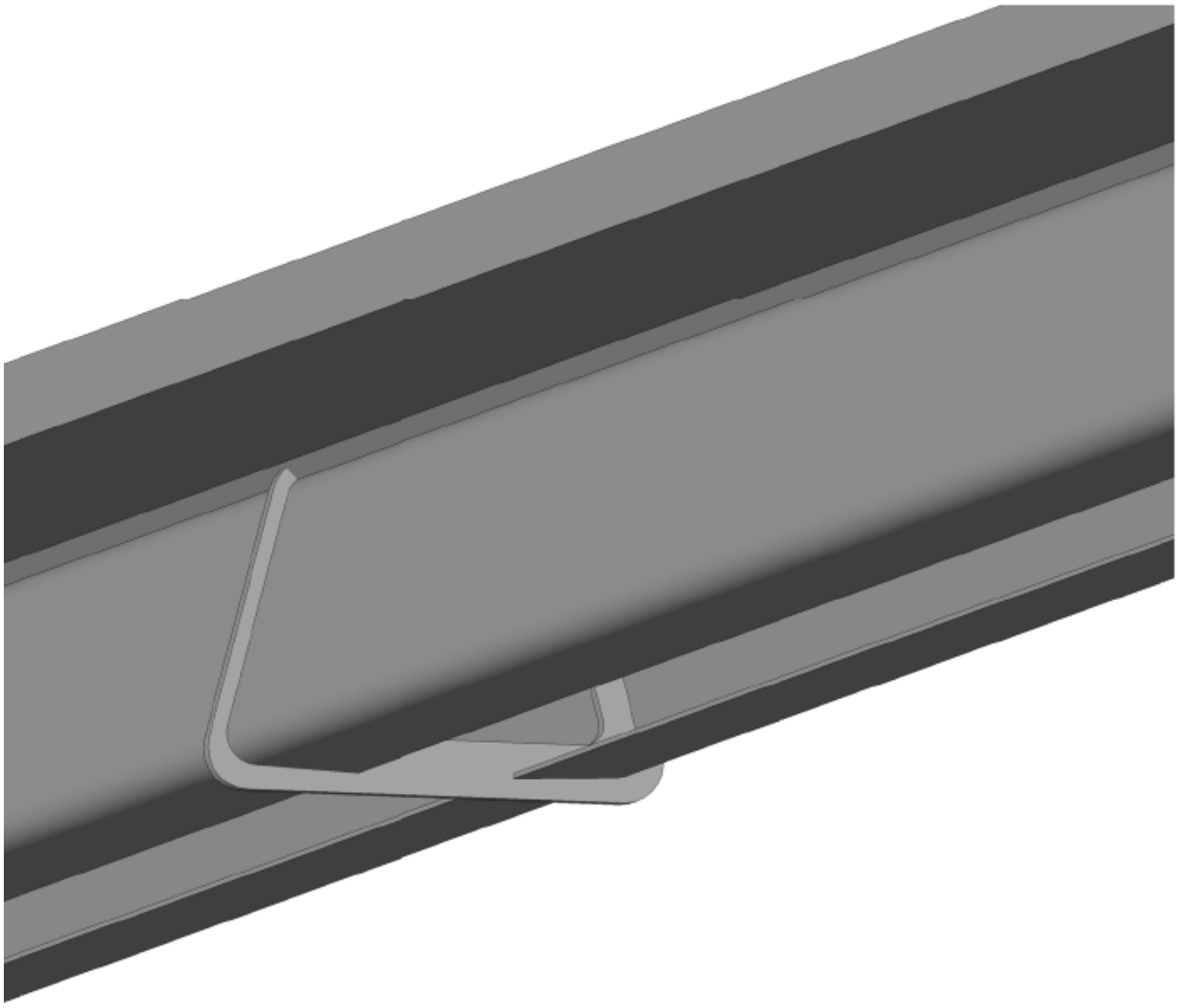

Figure 10. Initial Direct Weld Model

2.5 Direct Weld with Fill Plate

Based on the results of analyses attempting to smooth the transition at the splice plate, it was ultimately decided to return to the fill plate. The fill plate is a segment of plate that fills the gap between the bottom flanges near the splice plate; see *Figure 11*. The fill plate welds directly to the splice plate itself and drags the load back into the flanges through shear.

A major parameter the influences the behavior is the length of the fill plate. This is investigated in the following section.

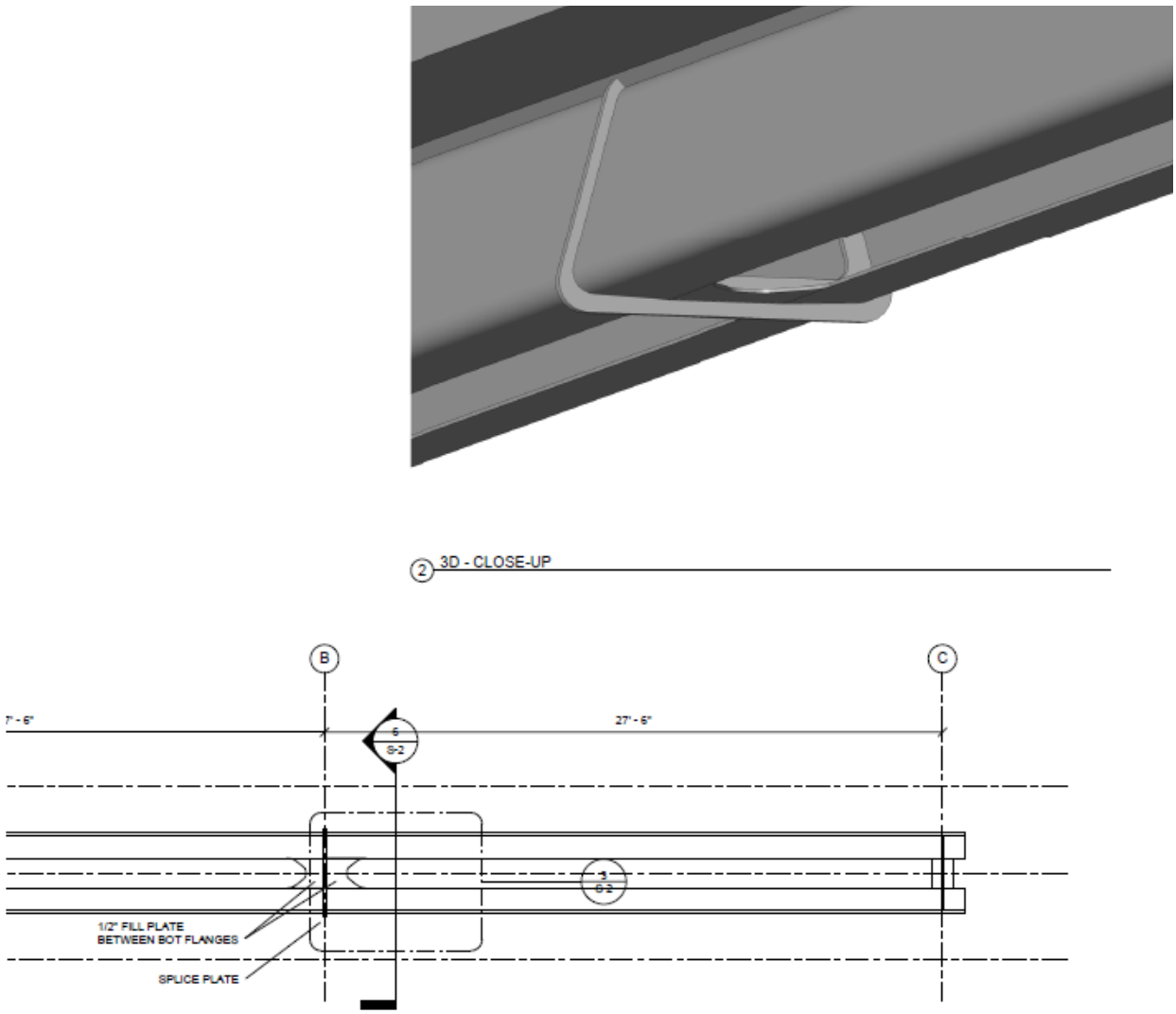

Figure 11. Fill Plate in Direct Weld Configuration

A series of analyses was run with varying lengths of plates. For each case, an initial elastic analysis was performed to evaluate the local stress concentrations followed by a full non-linear analysis to investigate the ultimate behavior.

Both the elastic and inelastic analysis used a loading equal to three (3) times the HL-93 loading. This was done to ensure the loading was large enough to produce an inelastic response. Since the elastic result is directly proportional throughout, service load stresses can be obtained by dividing the results by a factor of three. Note that the loading applied is a full lane so the results must be adjusted by the multiple presence factor. Finally, since the loading includes the lane load, the elastic stress result is not the fatigue loading.

2.5.1 Short Plate (Case e)

The short plate leaves a region of low stress near the middle (across the width). The cause is due to shear lag; insufficient length to transfer load. As such, more load is carried directly by the

flanges. This is evidenced by the low level of stress near the center of the plate in the *Figure 12* (1,698 KSI).

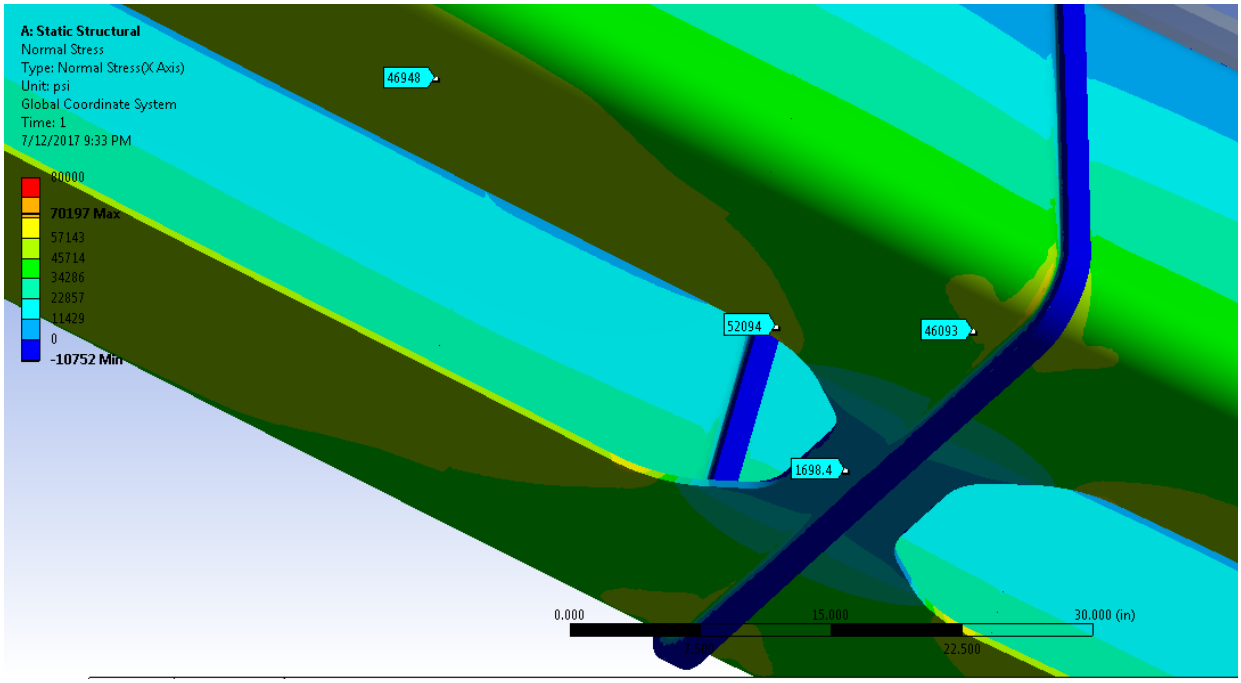

Figure 12. Short Plate (Case e)

The inelastic result is shown in *Figure 13*. The figure shows the equivalent plastic strain. The chart shows the maximum value (y-axis) versus time (x-axis). Time=1.0 corresponds to full load (3x HL-93).

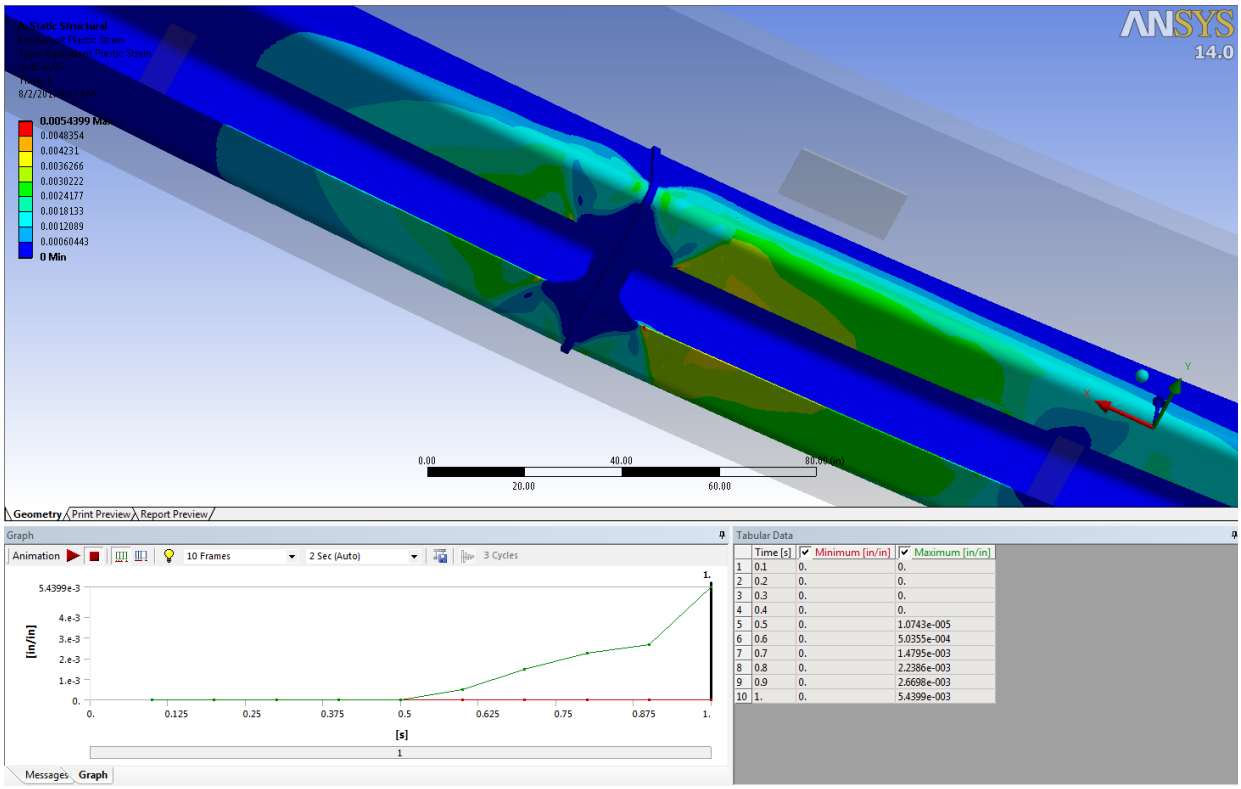

Figure 13. Short Plate (Case e) - Inelastic

2.5.2 Medium Plate (Case f)

As the plate is made longer, more load is dragged into the filler plate and the stress near the middle increases. The load carried by the flange decreases. Note that the stress near the middle of the plate has increased to 11,876 ksi (from 1,698 ksi), shown in *Figure 14*.

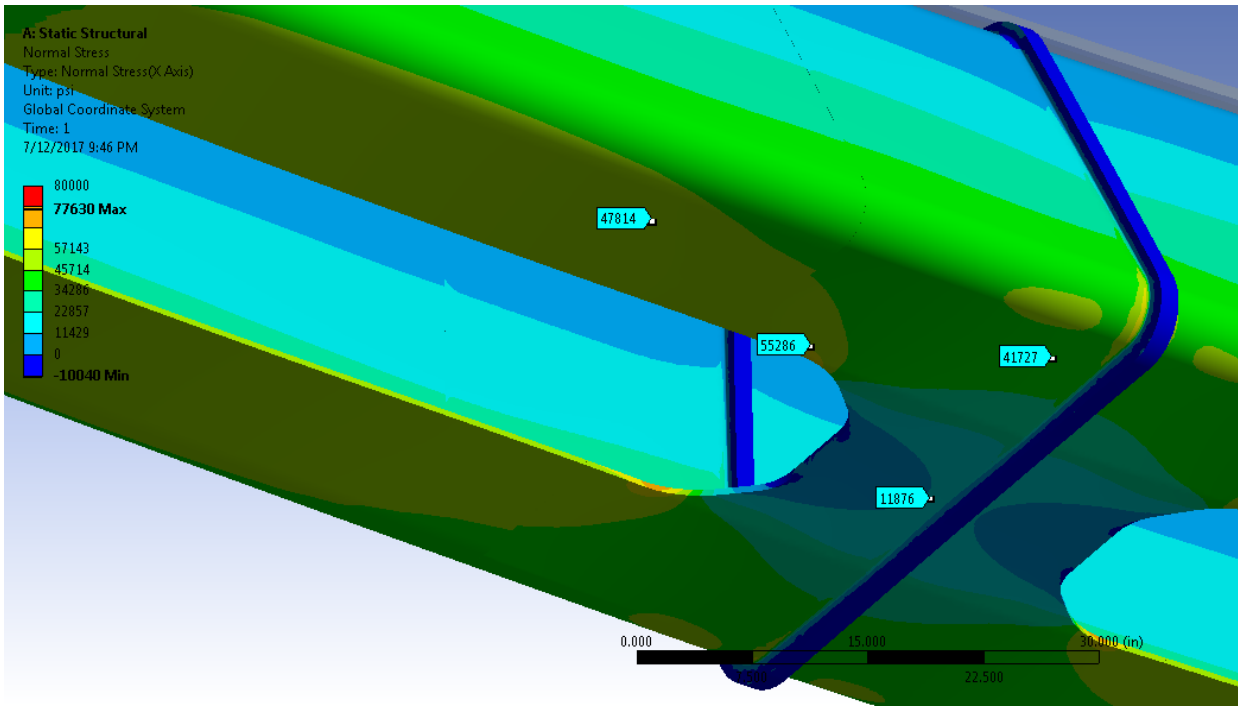

Figure 14. Medium Plate (Case f)

Inelatic analysis results in *Figure 15* shows a similar pattern with a slightly larger strain 7.9x10-3 verus 5.5x10-3.

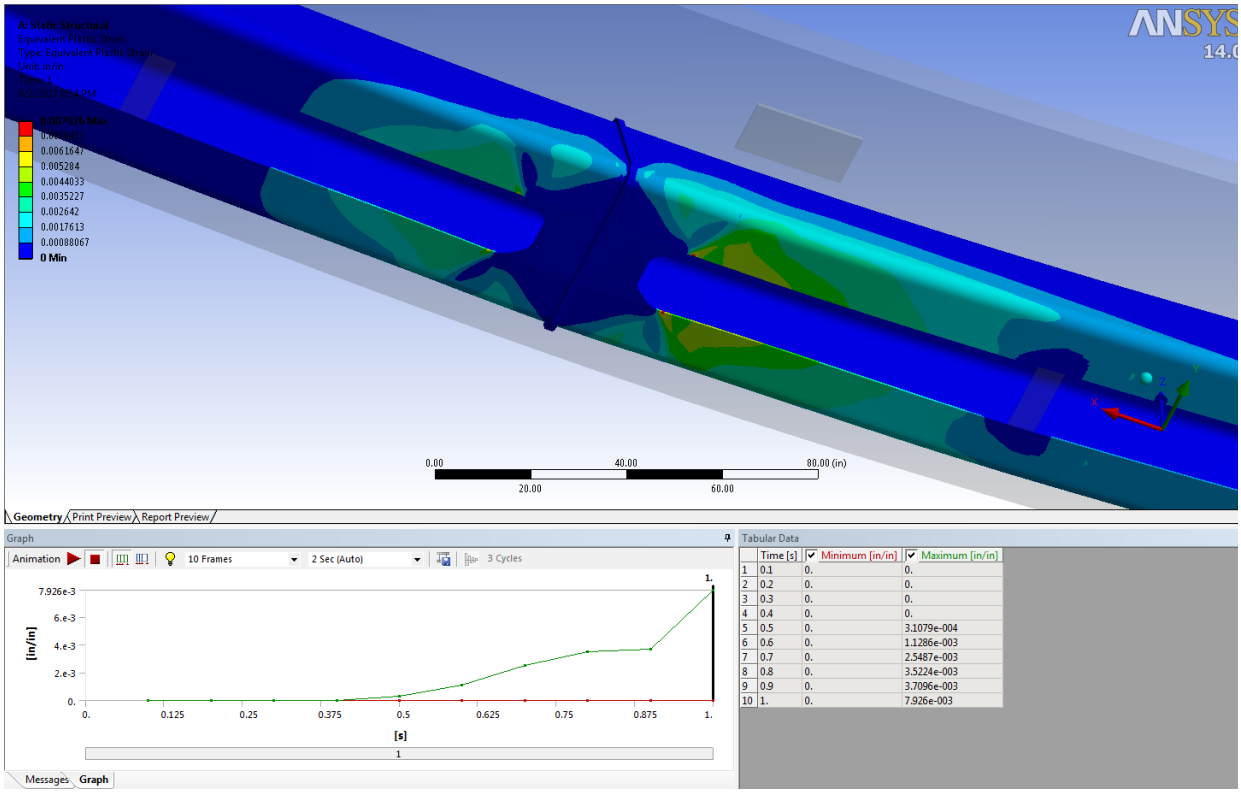

Figure 15. Medium Plate (Case f) - Inelastic

2.5.3 Long Plate (Case g)

With a very long fill plate, shown in *Figure 16*, the stress becomes more uniform across the width. However, since there is more load being dragged into the filler plate, the stress at the terminus of the filler plate increases (stress concentration).

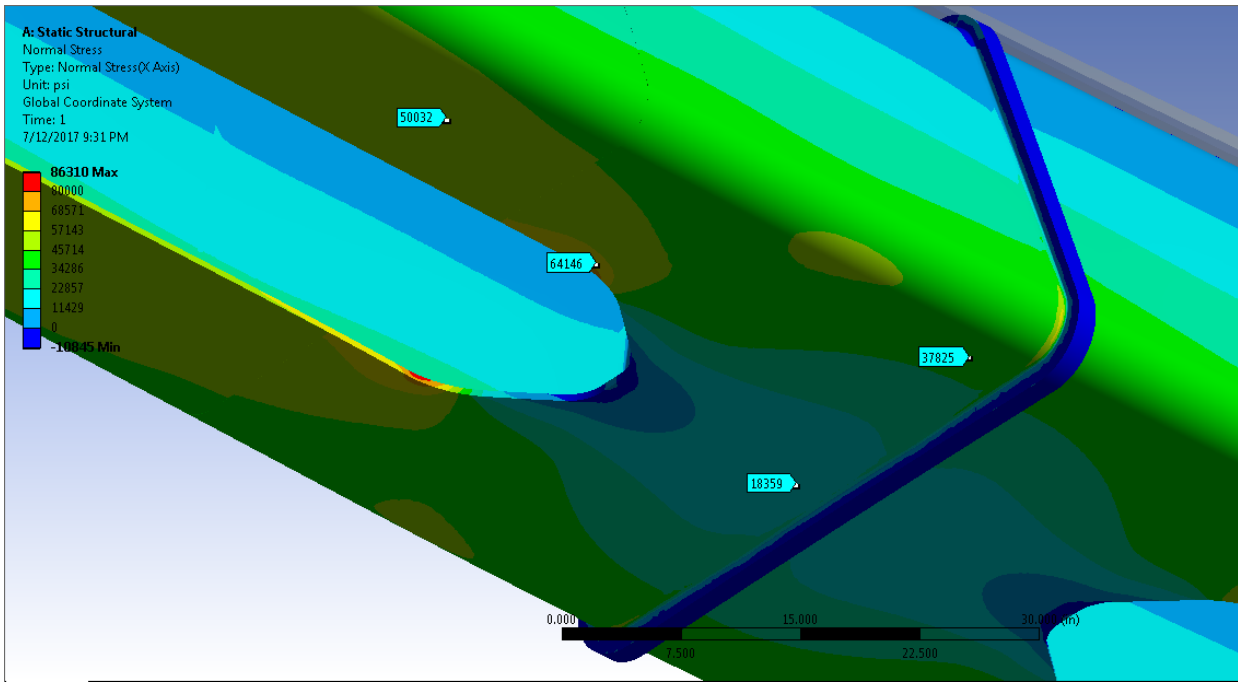

Figure 16. Long Plate (Case g)

Inelastic analysis (*Figure 17*) again shows an increase in plastic strain over the shorter plates.

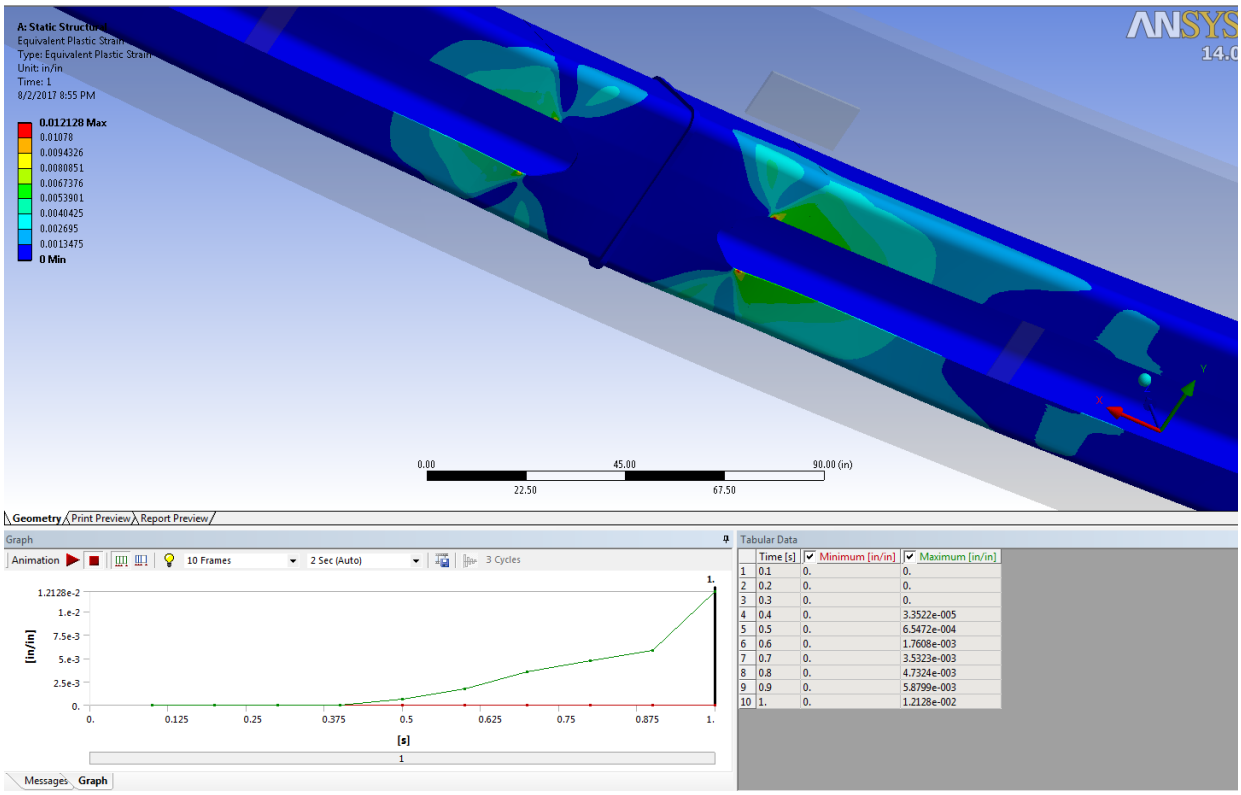

Figure 17. Long Plate (Case g) - Inelastic

2.5.4 Load Deflection – Comparison of Results

The load deflection results obtained from the inelastic analyses are shown in *Figure 18*. All of the cases described above are clustered with the similar behavior. Those with a different response are the base all shell models with no splice (3 models), which gave a slightly stiffer response; and one older model where there was no fill plate (Specimen 8), which gave a softer response (more deflection).

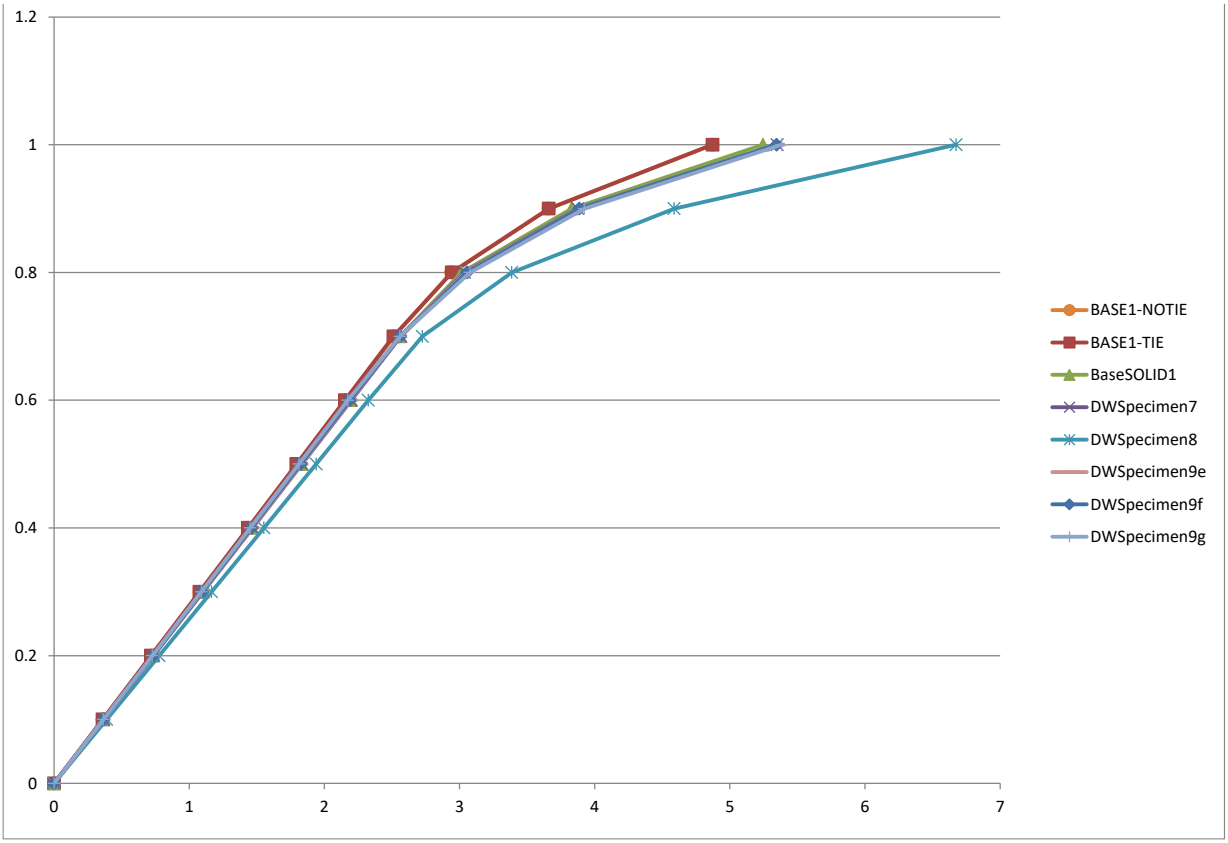

Figure 18. Load Deflection Results

(x-axis is inches of deflection, and y-axis is the load increment with a value of 1.0 corresponding to the same load value for all runs)

2.6 Effect of Flange Offset – Fabrication Tolerance

Figure 19 shows the results from a series of analyses where some fabrications offset has been considered. The flanges of the model on the left are perfectly in line. The flanges of the model on the right are offset by 1/8 inch; one fourth of the flange thickness. The right hand flange is down lower than the left hand flange. To equilibrate, the splice plate rotates in order to allow the centroid of the flanges to come into alignment under load. This creates localized bending in the flange and torsional stresses in the splice plate. However, it would appear the magnitude of these stresses are within reason for the amount of offset considered.

One simple solution to eliminate the concern of offset is to ensure alignment at the bottom flanges, where the tension transfer occurs, and allow any misalignment to occur at the top flange. Due to the presence of the slab and shear studs, the top flange is more accommodating of misalignment.

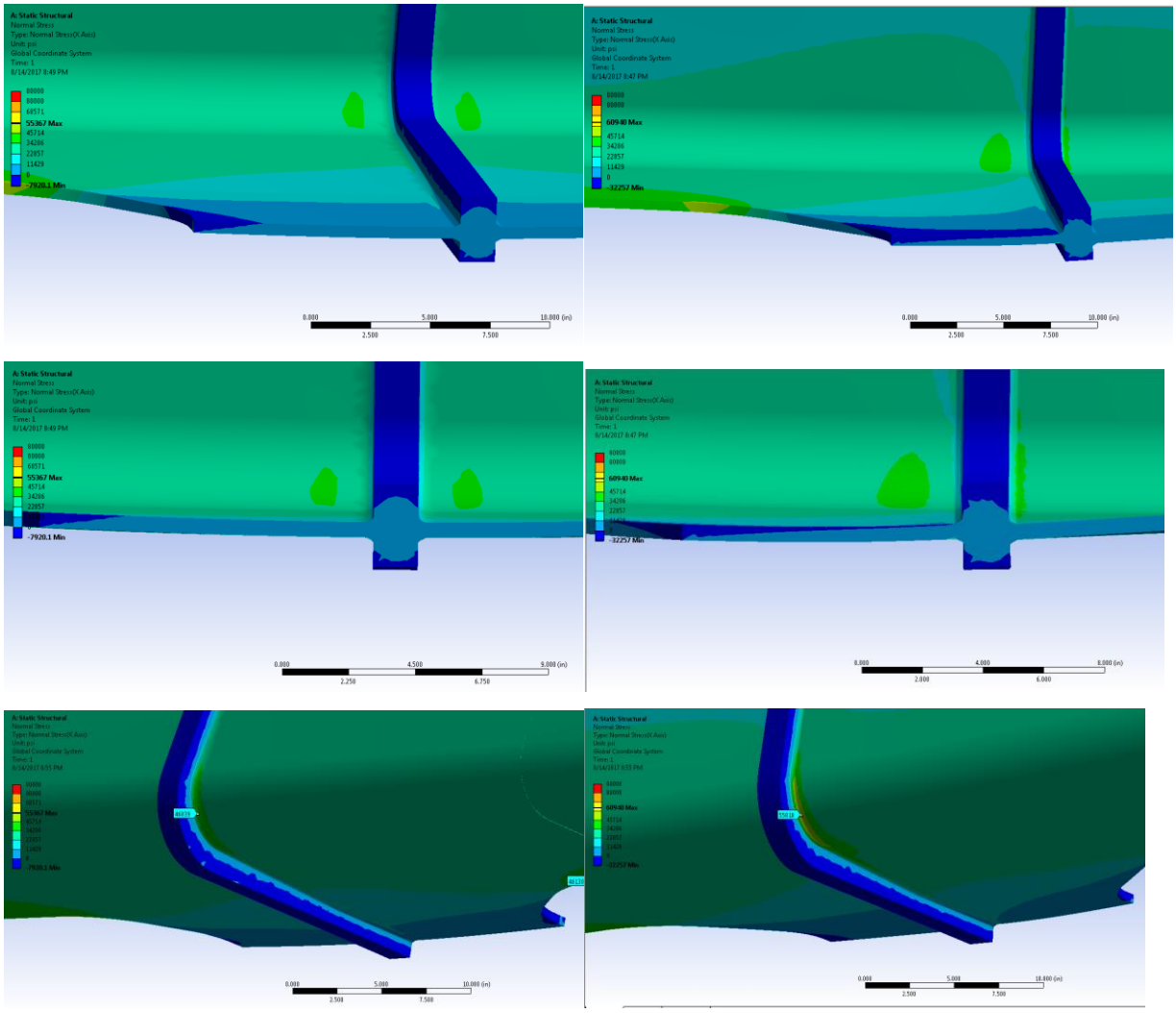

Figure 19. Misalignment Analysis Results

CHAPTER 3: CYCLIC TESTING

A full-scale test specimen was constructed to evaluate the performance of the spliced girder system under cyclic loading. Once the cyclic test was completed, the same specimen was used to perform an ultimate load test.

The total length of the specimen was 40 feet with a splice located at the middle of the span. The ends were supported 6 inches from each end for span length of 39 feet.

3.1 Specimen Construction

To allow for the loading apparatus and inspection of the girder during the test, the specimen had to be elevated about 7 ft. above the ground. To achieve that, end supports were constructed with sufficient height to provide the required clearance for inspection and sufficient width to provide stability for the test specimen. *Figure 20* shows the formwork and complete casting of the end supports. The final height of the end supports was determined to accommodate the following, (1) human height for inspection and instrumentation attachment, (2) the ceiling height of the lab, (3) crane range, and (4) the height of test apparatus. *Figure 21* shows the test specimen placed on top of the end supports.

Figure 20. Construction of end supports

Figure 21. Placement of FPG on top of the end supports

Scaffolding was placed on both sides of the girder to support the overhanging portion of the slab during casting. Wooden formwork for the deck slab was designed accordingly and placed on top of the scaffolds, as shown in *Figure 22.* Scaffolding was also used under the girder to fully support the weight of beam and we concrete. This replicates the casting of full depth deck panel on top of the FPG in precast plants with shored construction.

Figure 22. Placement of FPG on top of the end supports

Subsequently, the deck steel reinforcement was placed as designed. #5 bars @ 12” c/c both directions were provided at the bottom and #4 bars @ 12” c/c both directions were provided at the top as shown in *Figure 23*. Plastic chairs were used to ensure that reinforcement stayed in position during deck casting.

Figure 23. Placement of FPG on top of the End Supports

Figure 24 shows the final specimen. The average thickness of the deck slab was found to be 9.5 in. after casting. The sectional properties were revised for displacement ranges required during the fatigue testing since the original specimen design assumed 8 in. deck thickness. A spacer beam was placed between the top of the deck and the loading beam prior to testing.

Figure 24. Final test specimen.

3.2 Loading Protocol

Cycling loading was applied to the girder in the form of a sinusoidally varying point load located at midspan. The following sections describe how the number of cycles to be applied was determined.

3.2.1 Fatigue Resistance Equation

The applied fatigue stress range $(\Delta F)_n$ is inversely proportional to the cubic root of the number of cycles according to AASHTO-LRFD (Eq. 6.6.1.2.5-2) as shown in *Figure 25*. The term (N) is the Number of cycling loading that bridge will be subjected to during its design life, which is assumed to be 75 years. The value of N can be calculated according to AASHTO-LRFD (Eq. 6.6.1.2.5-3).

The term (A) is a fatigue constant that is based on the weld category in AASHTO-LRFD (Table 6.6.1.2.5-1). The term (n) is the number of stress range cycles the bridge experiences per truck passage based on AASHTO-LRFD (Table 6.6.1.2.5-2). For short span bridges, the value of n is 2. $(ADTT)_{SL}$ is the number of trucks per day in a single lane averaged over the design life specified in AASHTO-LRFD (Article 3.6.1.4).

$$(\Delta F)_n = \left(\frac{A}{N}\right)^{\frac{1}{3}} \qquad (6.6.1.2.5\text{-}2)$$

in which:

$$N = (365)(75)n(ADTT)_{SL} \qquad (6.6.1.2.5\text{-}3)$$

where:

A = constant taken from Table 6.6.1.2.5-1 (ksi^3)
n = number of stress range cycles per truck passage taken from Table 6.6.1.2.5-2
$(ADTT)_{SL}$ = single-lane $ADTT$ as specified in Article 3.6.1.4

Figure 25. Fatigue life equation from AASHTO-LRFD.

The resulting calculation of N for the prototype bridge is shown below. The assumed daily traffic (ADT) is 20000 with 20% of that traffic being trucks with only one lane available resulting in an $ADTT_{SL}$ of 4000.

N = 75*365*2*4000 = 219,000,000

3.2.2 Simulation of AASHTO Truck in Lab by Using S-N Curve

A typical bridge will be subjected to millions of cycles of truck loading. For example, using the equations listed in Figure 10, the number of times that trucks pass over a bridge during the 75-year design life would be 219,000,000.

Applying 219,000,000 would take a very long time. To shorten the cyclic test period and at the same time simulate the effect of truck traffic over a 75-years design life, the following relationship can be used to move along the S-N curve to determine the stress range (and necessary loading) required for a specified number of cycles. This also ensures that the chosen stress range is above the fatigue threshold value, below which the detail would have infinite life.

$$(\Delta F1)^3 * N1 = A$$

$$(\Delta F2)^3 * N2 = A$$

Now equating both equations:

$$(\Delta F1)^3 * N1 = (\Delta F2)^3 * N2$$

$$\Delta F1 = M1 * y/I \;\; \& \;\; \Delta F2 = M2 * y/I$$

Since the cross-sectional properties y & I remain the same, the equation can be simplified as follows:

$$\frac{M1}{M2} = \left(\frac{N2}{N1}\right)^{1/3}$$

Where:

M1= Moment produced by design truck

N1= Number of fatigue cycles induced over the design life of the bridge

M2= Magnified moment required to be applied to test specimen to Simulate AASHTO design truck for N2 cycles.

N2= Number of cycles to be applied to the specimen

3.2.3 Calculation of Load Applied

Using the relationship developed above, five million cycles were chosen to be applied to the specimen simulating 75-years design life for the bridge. This was achieved by applying higher loads at a lower number of cycles, as compared to 219,000,000 cycles at much less load. During each cycle, the resulting tensile stress at the bottom flange was about 10 ksi, as compared to about 2.5 ksi that would be induced in fatigue limit state II corresponding to 219,000,000 cycles of truck passage.

In short, applying 5,000,000 cycles of load, producing about 10 ksi in the bottom flange will be a point on S-N curve, the same way the point corresponding to 219,0000,000 cycle at about 2.5 ksi tensile stress. The point marked on the S-N curve is shown below in *Figure 26*. The interpretation is that if the connection performed as a Category C (or better), no failure would be expected. However, failure would be predicted if the detail performed as Category D (or less). Note that the relationship for moving along a curve is independent of the category (lines are parallel). The anticipated category is C (CJP weld T joint or butt splice without removal of weld reinforcement).

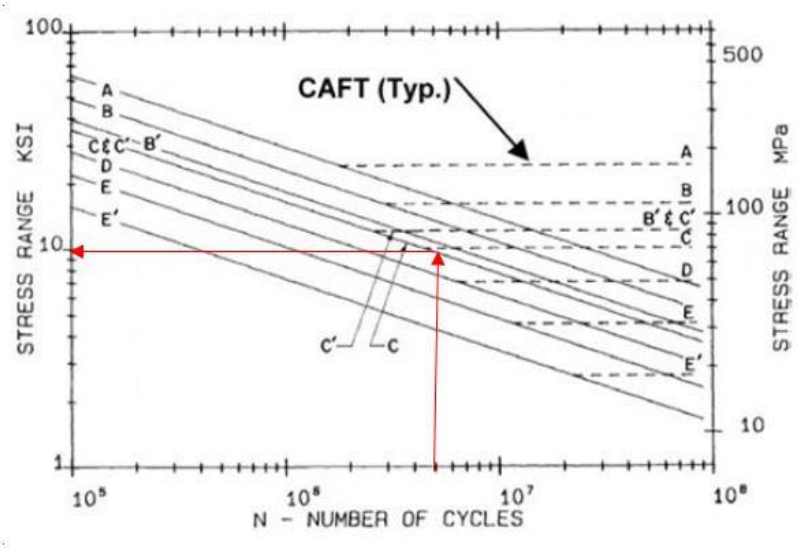

Figure 26. S-N Curve

Now calculating moment induced by HS20 truck on the bridge having span L=39 ft., tested in this study:

The Live Load Distribution Factor = 0.662

Load Factor for Fatigue= 0.75

Bending Moment Produced by HS20 Truck, M1= 192.2 K-ft

No. of desired cycles for experiment, N2= 5,000,000 & N1= 219,000,000

Using the equation, M2 can be calculated, as well as the required point load at midspan:

$$\frac{M1}{M2} = \left(\frac{N2}{N1}\right)^{1/3}$$

M_2= 669 K-ft

$P= 4*M_2/L$

$P= 69$ Kips

3.3 Instrumentation – Fatigue Test

3.3.1 Strain Gauges

The test specimen was extensively instrumented to monitor possible changes in its behavior due to formation of fatigue cracking or another local failure. The data collected was used to evaluate the weld and specimen behaviors. Visual inspection of weld conditions was also performed at regular time intervals. *Figure 27* shows the layout of the strain gauges. The plan view shows four sections at which strain gauges were installed. Steel strain gauges were applied on the girder at two locations near mid-span (opposite sides of the weld), adjacent to welds, and at a quarter of the span each side. The blowup in *Figure 28* shows the strain gauges applied at mid-span on one side of the weld. The denotation ML refers to middle left. Twelve strain gauges were applied on each side across the weld. In total 44 steel strain gauges were applied. In addition to the steel strain gauges, four embedded vibrating wire strain gauges were placed inside the concrete deck. Three surface strain gauges at the top of the deck slab at mid-span were also attached as shown in section A-A.

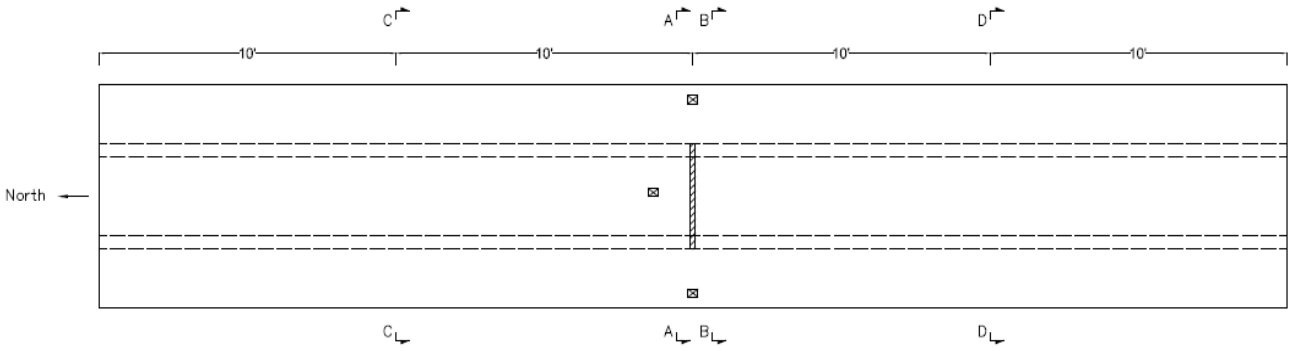

Figure 27. Strain Gauge Layout Plan

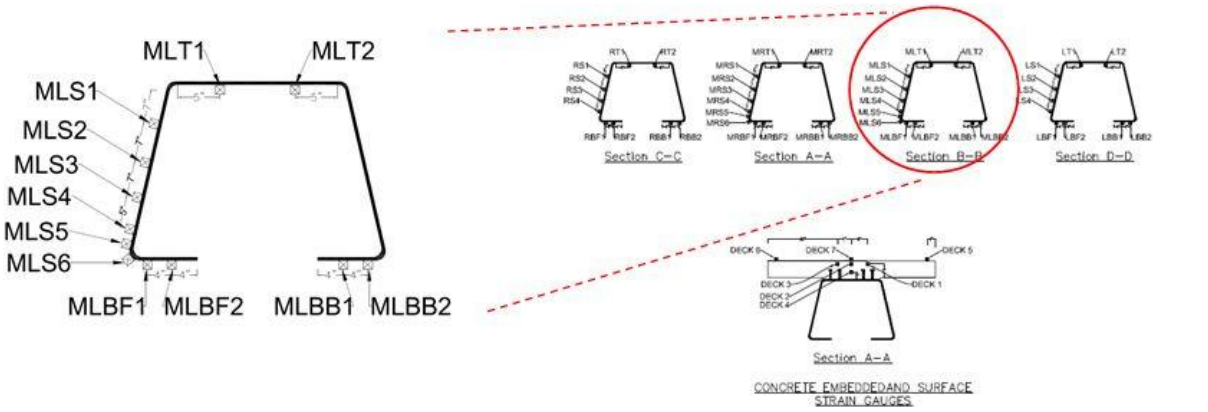

Figure 28. Strain Gauge Layout Cross Section.

3.3.2 Potentiometers

Global behavior of the test specimen was also monitored by measuring the specimen deflection at several points. Potentiometers were deployed to measure the deflections of the girder at three locations: mid-span and each quarter point. Girder ends were placed on an elastomeric pad that allowed for some compression. Therefore, there was also deflection at girder ends necessitating measurements at these locations. The schematic elevation and section with applied string potentiometers are shown in *Figure 29.*

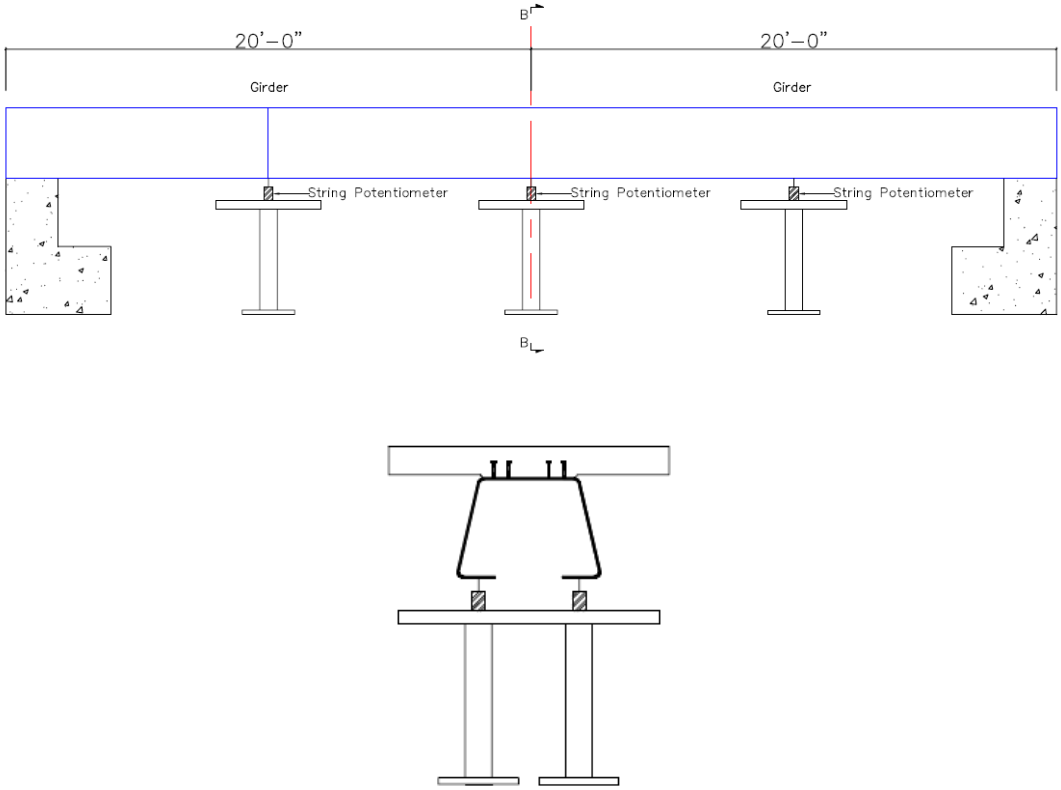

Figure 29. Potentiometer Layout, Elevation and Section.

3.4 Fatigue Test Results

3.4.1 Strain Results

Data from strain gauges placed at various locations were recorded and analyzed. *Table 3* shows the range of strains against the range of force applied along the course of the experiment. This result is shown for the strain gauge at bottom flange located at mid-span on the left side of the weld. *Figure 30* is the graphical representation of the range of strains along the course of the experiment.

3.4.2 Analysis of the Results

Based on calculations carried out before the experiment, The applied load corresponding to the desired tensile stress (10 ksi) and strain was known. These values fluctuated slightly during the test. However, no major sudden changes nor progressive changes that would indicate a failure or significant degradation of the specimen capacity or stiffness were apparent. The observed variations are likely due to minor changes to boundary conditions, thermal effects, and sensor drift. *Table 3* depicts the deviation of strain range from expected values. It can be seen that the difference remained less than 4% throughout the test.

Table 3. Range of strains along course of experiment for MLS4.

LOCATION OF SENSOR	NO. OF CYCLES (M)	RECORD	RANGE OF LOAD (KIP)			EXPECTED STRAIN DIFFERENTIAL	RANGE OF STRAIN (με)			% DIFF-STR EXPECTED-STR
			MIN	MAX	DIFF		MIN	MAX	DIFF	%
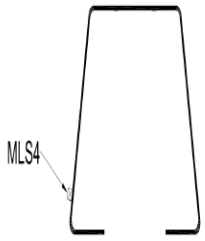	0.17	AFTER	6.3	81.0	74.7	344.0	28	372	344	0.00%
	0.55	AFTER	6.6	81.0	74.4	342.6	30	374	344	0.40%
	0.80	AFTER	5.3	76.0	70.8	325.8	22	360	338	3.74%
	1.05	AFTER	5.1	76.8	71.7	330.2	23	358	335	1.46%
	1.40	AFTER	4.2	75.0	70.8	326.0	20	350	330	1.21%
	1.55	AFTER	6.5	79.5	73.0	336.2	40	380	340	1.14%
	1.90	AFTER	7.3	80.0	72.7	334.8	30	377	347	3.65%
	2.25	BEFORE	7.0	79.0	72.0	331.6	27	366	339	2.24%
		AFTER	6.5	81.0	74.5	343.1	28	370	342	-0.31%
	2.50	BEFORE	5.0	78.0	73.0	336.2	19	361	342	1.73%
		AFTER	6.0	78.0	72.0	331.6	21	362	341	2.85%
	2.75	BEFORE	6.5	79.0	72.5	333.9	39	380	341	2.14%
		AFTER	7.0	79.0	72.0	331.6	38	380	342	3.15%
	3.15	BEFORE	6.0	78.0	72.0	331.6	33	378	345	4.05%
		AFTER	6.7	78.0	71.3	328.3	36	379	343	4.46%
	3.45	AFTER	7.0	78.0	71.0	327.0	40	380	340	3.99%
	3.75	BEFORE	5.0	77.0	72.0	331.6	27	370	343	3.45%
		AFTER	5.5	76.5	71.0	327.0	30	370	340	3.99%
	4.10	BEFORE	5.0	76.7	71.7	330.2	24	365	341	3.28%
		AFTER	5.5	76.5	71.0	327.0	27	365	338	3.38%
	4.30	BEFORE	5.0	75.5	70.5	324.7	30	370	340	4.73%
		AFTER	5.0	75.5	70.5	324.7	33	370	337	3.80%
	4.60	BEFORE	5.0	75.5	70.5	324.7	35	372	337	3.80%
		AFTER	5.0	76.0	71.0	327.0	35	372	337	3.07%
	5.00	BEFORE	3.7	74.0	70.3	323.7	16	352	336	3.79%

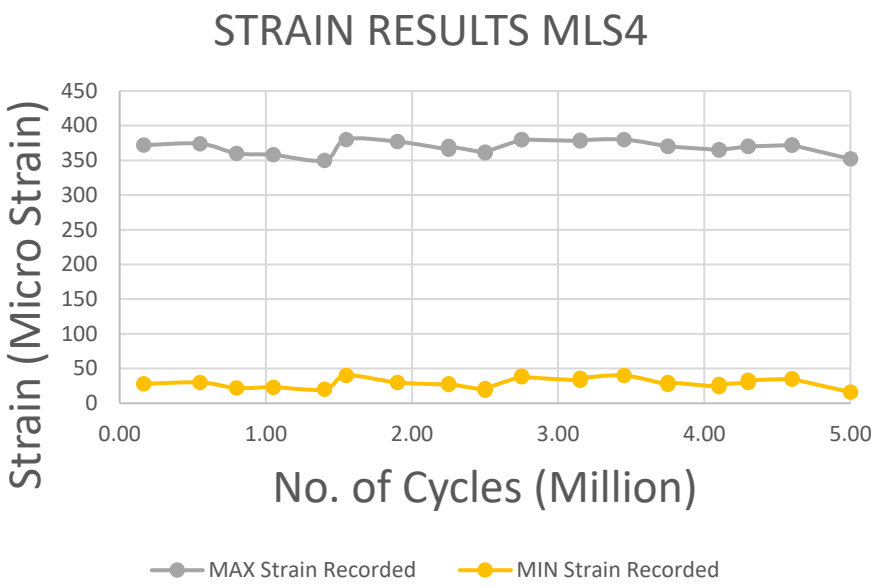

Figure 30. Range of strains along course of experiment for MLS4.

3.4.3 Strain Distribution Across Cross Section

Strain distribution through the cross-section of the bridge at mid-span is shown in *Figure 31*. The brown line shows the strain predicted from hand calculations. Other lines show the strains produced in the cross-section after every 1 million cycles were completed. It can be observed that the predicted values for tensile strain in the steel were in close agreement to those obtained from the testing. The linear strain distribution across the depth of the cross-section is an indication that full composite action was maintained throughout the test.

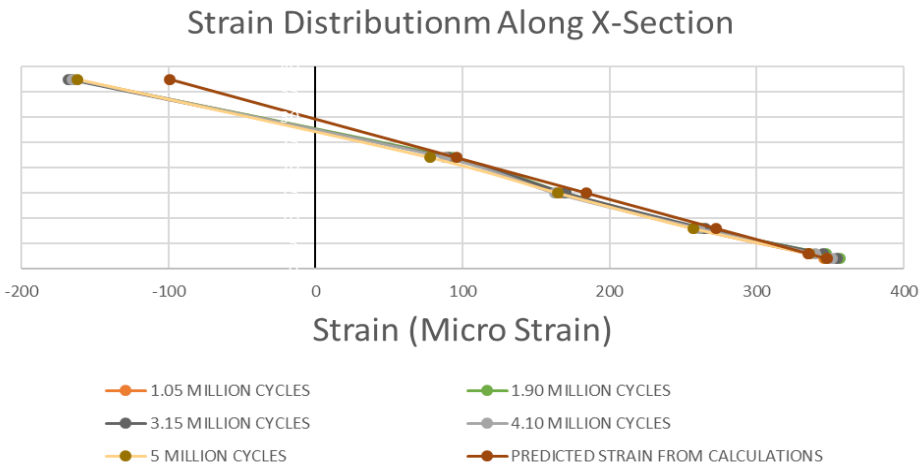

Figure 31. Strain Distribution across cross section of the bridge.

3.4.4 Stiffness

Apparent stiffness (load divided by displacement) of the specimen along the course of experiment is shown in *Figure 32*. A slight reduction of stiffness is observed apparent. However, the amount

was not significant and although the general trendline is sloped, the tail of the experimental results is fairly flat. Visual inspection was carried out after every 500,000 cycles through the course of the experiment and no visible cracks on steel girder was seen.

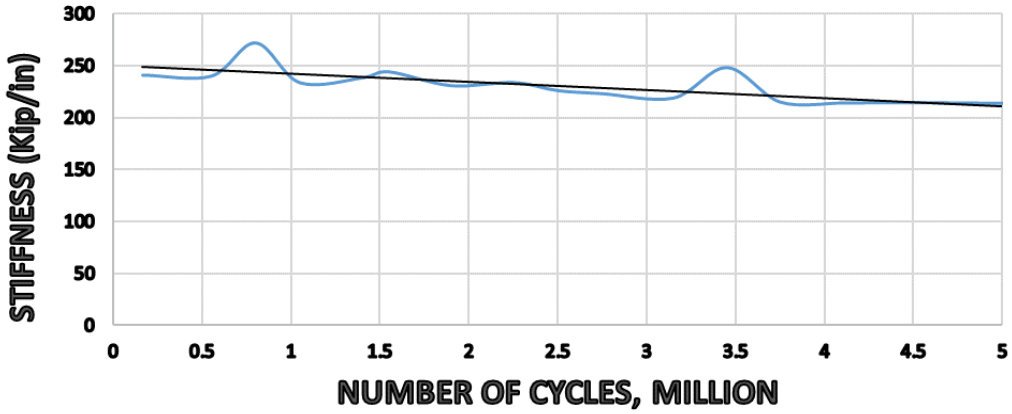

Figure 32. Stiffness variation throughout the duration of the experiment.

CHAPTER 4: ULTIMATE TEST

An ultimate load test was conducted in November 2020 to determine the ultimate load capacity of the folded plate girder. The test was conducted as 4-point load test and is shown below in *Figure 33.*

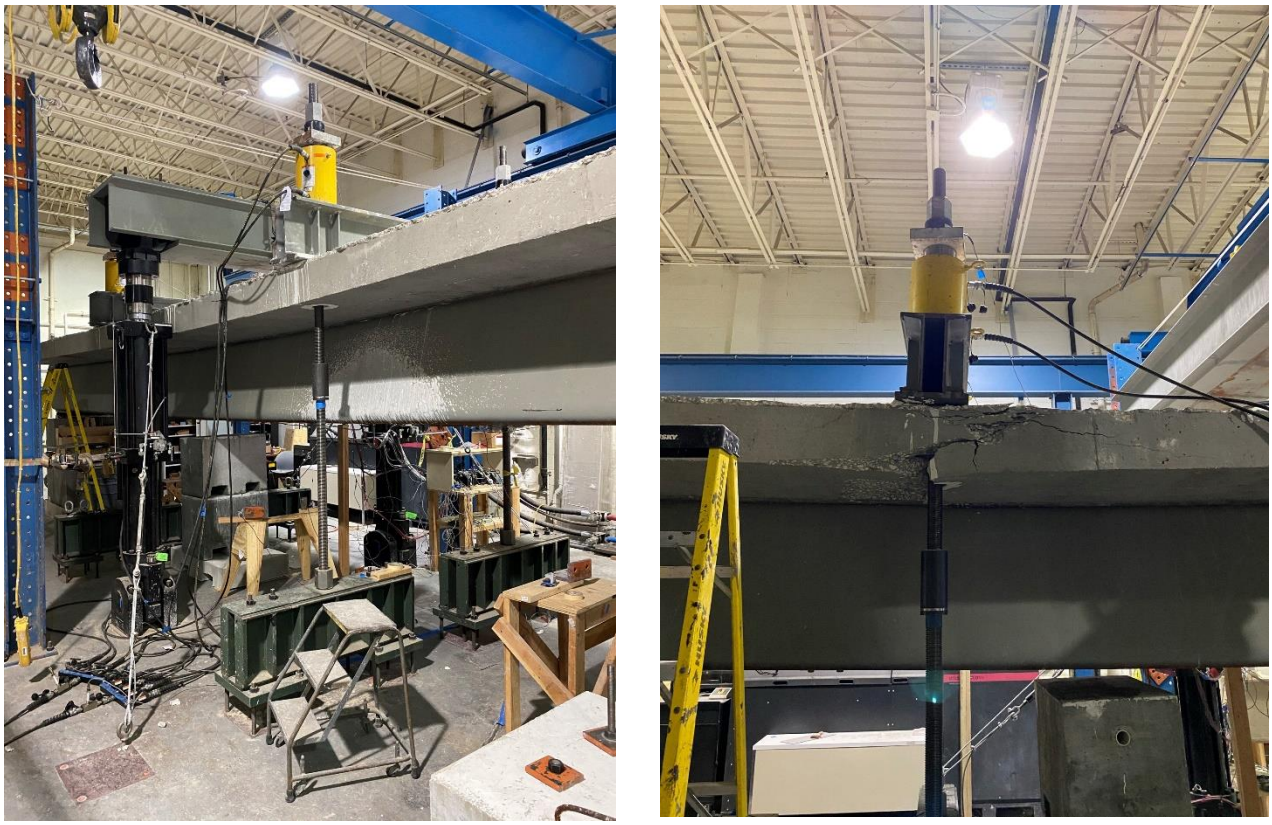

Figure 33. Ultimate Load Test Setup for Folded Plate Girder.

4.1 Predicted Capacity

To forecast the moment capacity of the composite section of folded plate girder with concrete deck, a moment curvature analysis was performed. The composite section is shown in *Figure 34*. The moment curvature curve is shown below in *Figure 35*. The maximum moment capacity calculated was 68932 Kip inches and the ultimate load predicted was 820.62 Kips.

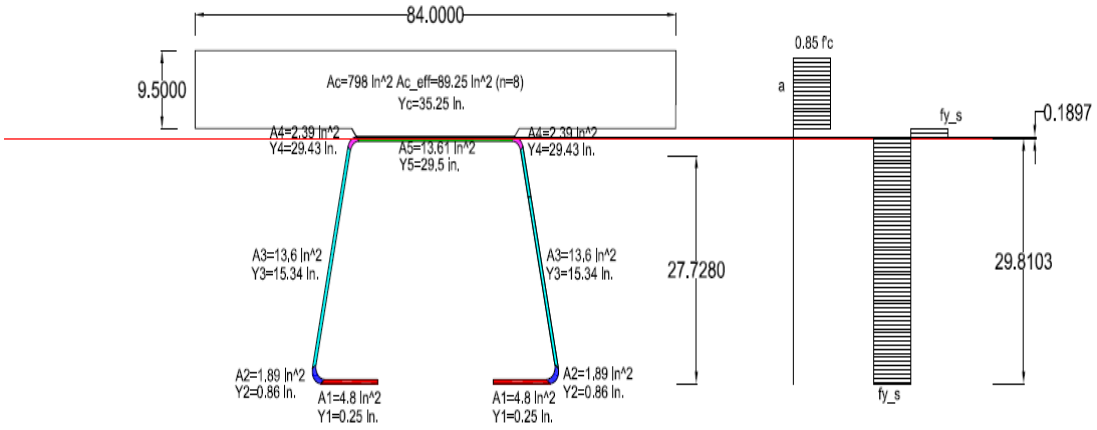

Figure 34. Composite Section of the Tested Bridge.

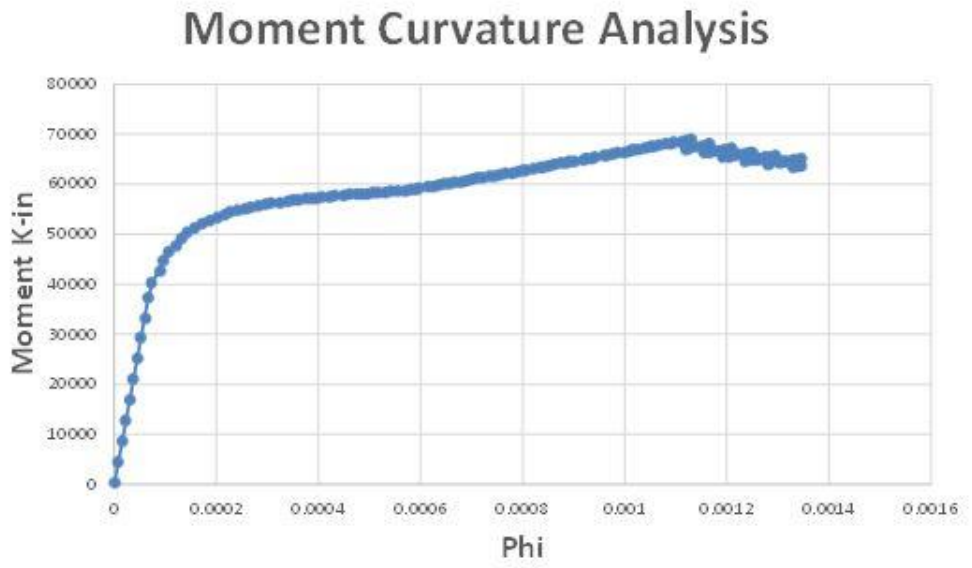

Figure 35. Moment Curvature Analysis.

4.2 Instrumentation – Ultimate Test

4.2.1 Strain Gauges

The instrumentation plan was like the one shown above in *Figure 28* except for the addition of two more strain gauges on the connection plates which are joining the bottom flanges of the folded plate girder. The strain gauge setup used for the ultimate test is shown below in *Figure 36 and Figure 37.*

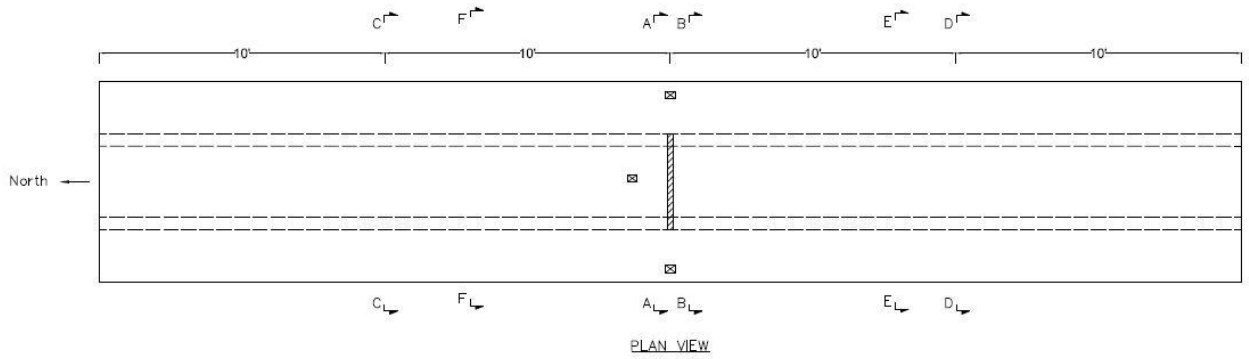

Figure 36 Strain gauge layout in plan for ultimate test.

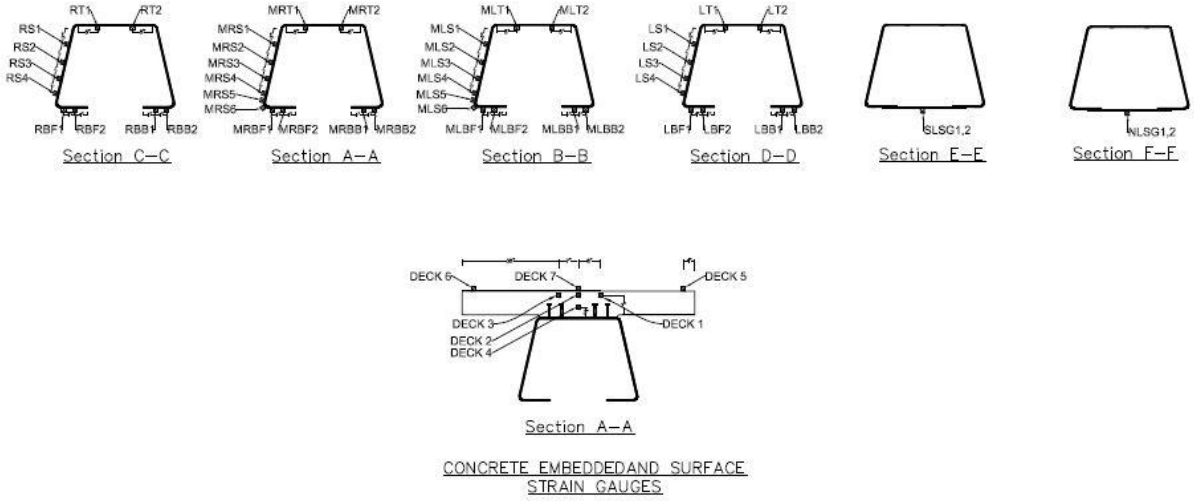

Figure 37. Strain gauge layout in section for ultimate test.

4.2.2 Potentiometers

The same potentiometer setup was used for the ultimate test, however there was an additional potentiometer attached with the deck slab to monitor and compare the deflection of deck slab with the folded plate girder. The section view of the deployed potentiometers is shown below in *Figure 38.* The potentiometers are denoted as DM which means displacement at mid span, next part represents the location i.e. deck means displacement of the deck.

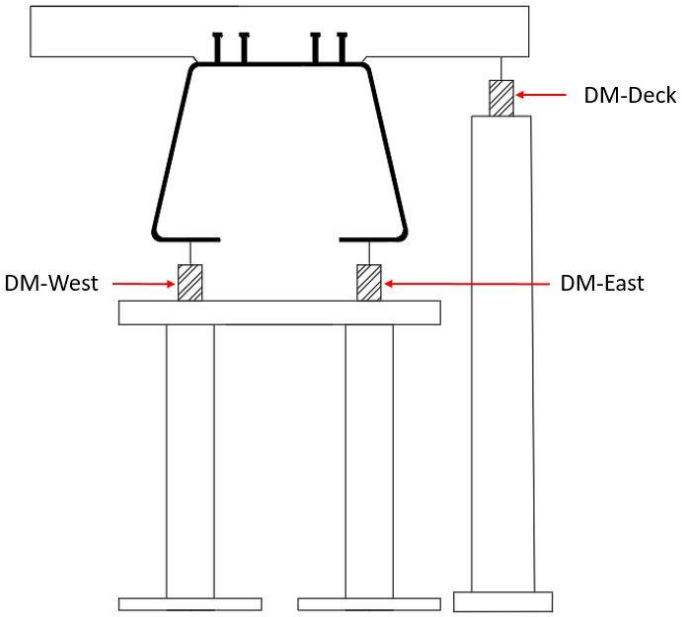

Figure 38. Potentiometer Setup, Ultimate Test

4.3 Ultimate Test Results

4.3.1 Strain Results

Data from strain gauges placed at various locations were recorded during the ultimate test and analyzed. The variation in strain value against force for strain gauge MRS4 shown in *Figure 39* has been plotted below. It can be seen from the result that the load has been increased in intervals of loading and unloading. The result shows the maximum strain of about 10600 micro strains at about 893 Kips of load.

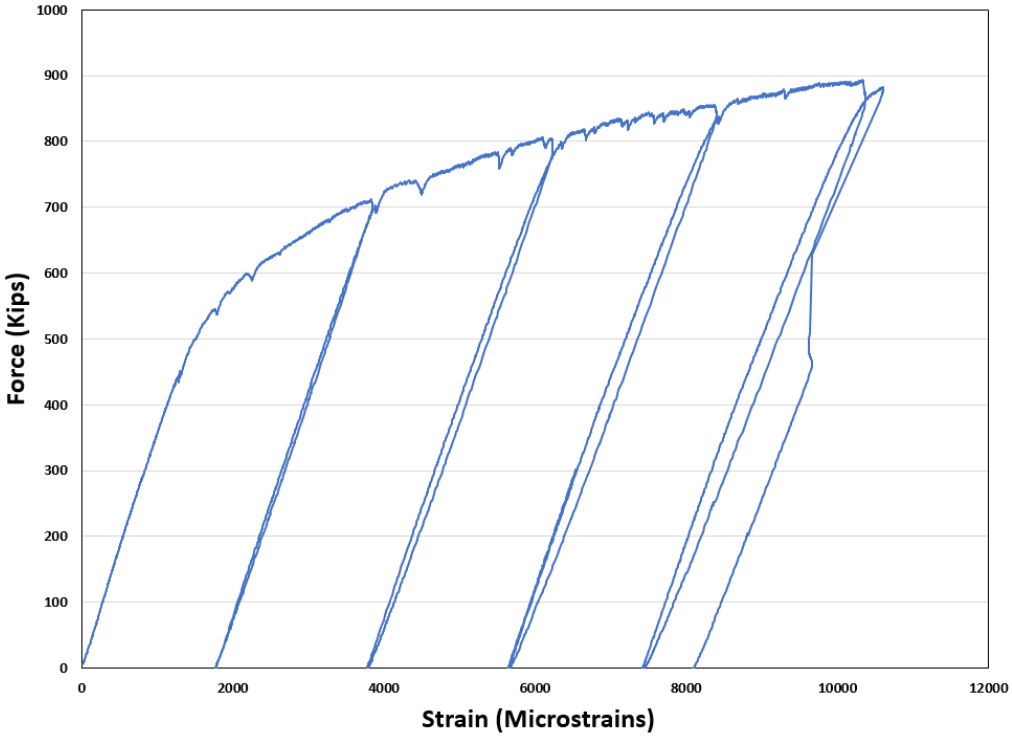

Figure 39. Load Vs Strain, strain gauge MRS4

4.3.2 Strain Distribution Across Cross Section

Strain distribution through the cross-section of the bridge at mid-span during ultimate load test is shown below in *Figure 40*. Each dot on respective line shows the location of the sensor along the cross section. Each line shows strain values in sensors at certain load i.e. 100 to 700 kips.

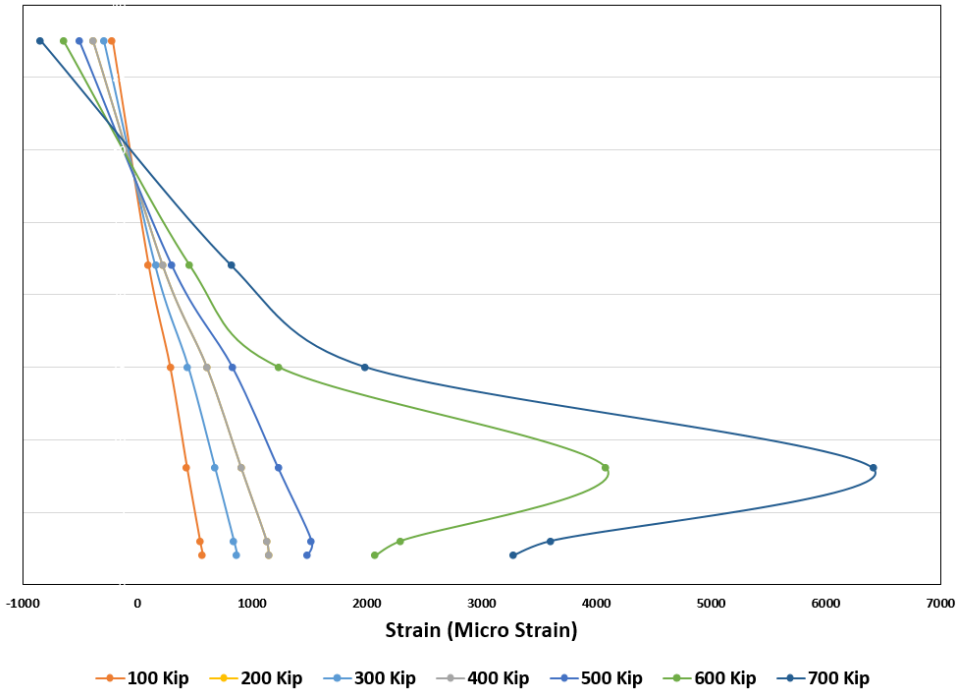

Figure 40. Strain Distribution Curve for loads 0-700 kips along X section

4.3.3 Load Deflection Results

The deflection measurements were taken during the ultimate test from potentiometers as shown above in *Figure 38*. The load deflection curve for deck slab and potentiometer DM west are shown below in *Figure 41 and Figure 42.*

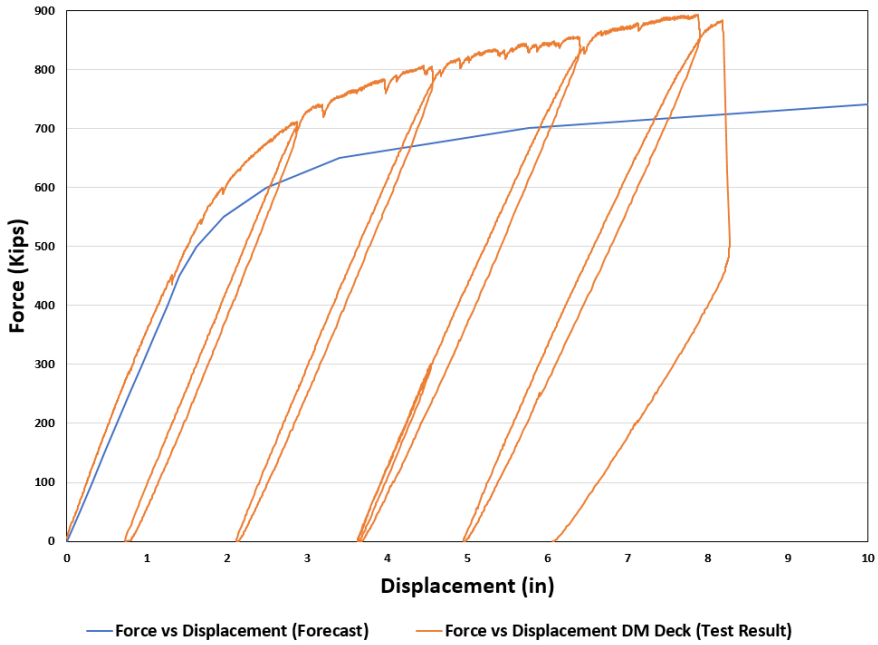

Figure 41. Comparison of Force vs Displacement, DM Deck with Forecast values.

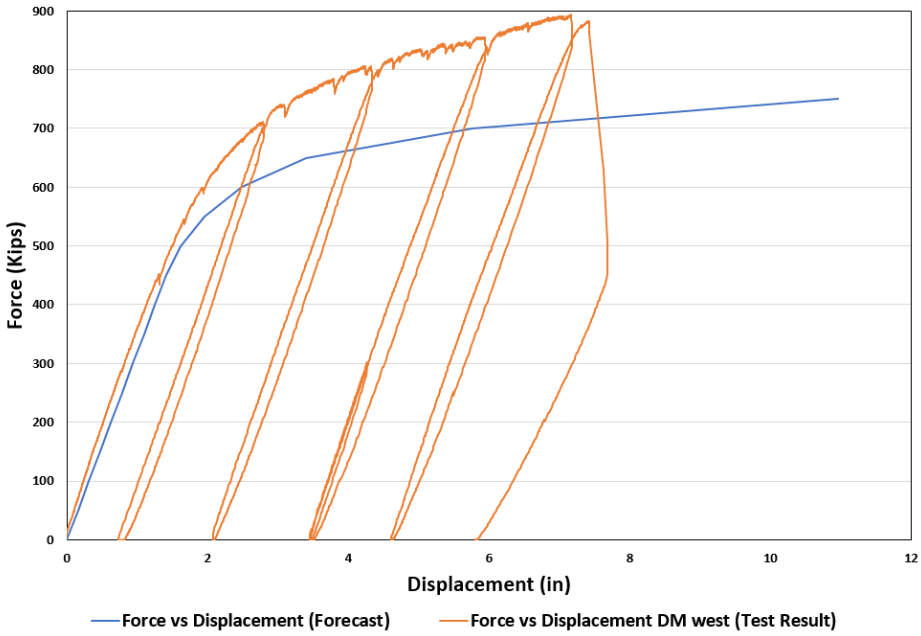

Figure 42. Comparison of Force vs Displacement, DM West with Forecast values

CHAPTER 5: CONCLUSIONS

The fatigue load test and ultimate test was conducted on a 40 feet span folded plate girder with cast in place concrete deck. The girder was spliced with a full penetration weld at mid span, as would be required to increase the span length of folded plate girders to over 100 feet.

The girder performed very well under the fatigue load in which five million cycles were applied. The fatigue load and number of cycles were applied simulating AASHTO truck passage over the bridge in 75 years of its design life. It was observed that there was no significant loss of stiffness during the fatigue load testing. The bridge was inspected after completion of every half million cycles and no damage or cracking was observed during inspection.

The bridge specimen was loaded until failure to determine the ultimate load of the specimen and to observe the failure pattern of the bridge. It was observed that the welded connection remained intact during ultimate test and the specimen failed due to crushing of concrete at points of load application in the deck. The cracked specimen is shown below in *Figure 43*. The ultimate load which was applied on the specimen was 893 Kips, the predicted ultimate load was about 821 Kips so the specimen behaved slightly better than forecasted.

Figure 43. Crushed Specimen after Ultimate Test.